JSC-29295

SPACE RADIATION CANCER RISK PROJECTIONS FOR EXPLORATION MISSIONS: UNCERTAINTY REDUCTION AND MITIGATION

FRANCIS A. CUCINOTTA[1], WALTER SCHIMMERLING[2], JOHN W. WILSON[3], LEIF E. PETERSON[4], GAUTAM D. BADHWAR[1], PREMKUMAR B. SAGANTI[1], AND JOHN F. DICELLO[5]

[1]*NASA, Johnson Space Center, Houston, TX 77058*

[2]*NASA, Headquarters, Washington, DC 20546*

[3]*NASA, Langley Research Center, Hampton, VA 23681*

[4]*Department of Medicine, Baylor College of Medicine, Houston, TX 77030*

[5]*Johns Hopkins University School of Medicine, Baltimore, MD 21287*

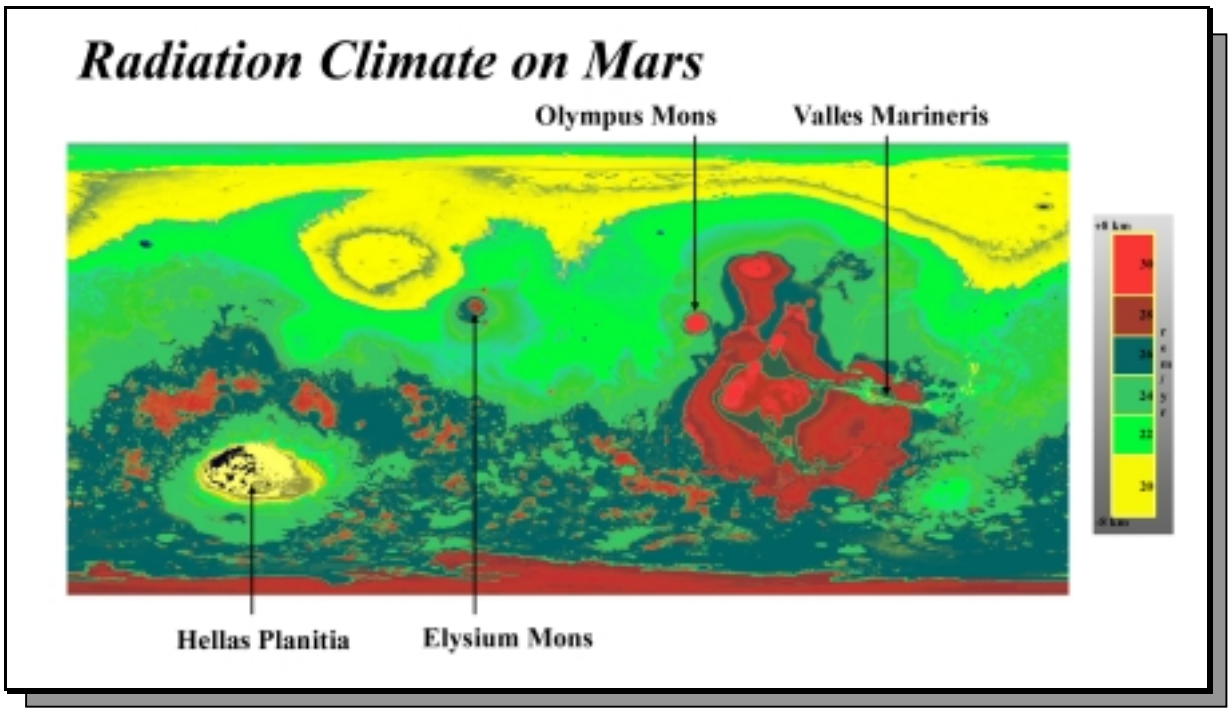

January 2001

SPACE RADIATION CANCER RISK PROJECTIONS FOR EXPLORATION MISSIONS: UNCERTAINTY REDUCTION AND MITIGATION

FRANCIS A. CUCINOTTA[1], WALTER SCHIMMERLING[2], JOHN W. WILSON[3], LEIF E. PETERSON[4], GAUTAM D. BADHWAR[1], PREMKUMAR B. SAGANTI[1], AND JOHN F. DICELLO[5]

[1]*NASA, Johnson Space Center, Houston, TX 77058*

[2]*NASA, Headquarters, Washington, DC 20546*

[3]*NASA, Langley Research Center, Hampton, VA 23681*

[4]*Department of Medicine, Baylor College of Medicine, Houston, TX 77030*

[5]*Johns Hopkins University School of Medicine, Baltimore, MD 21287*

ABSTRACT

Late effects from the high charge and energy (HZE) ions present in the galactic cosmic rays (GCR) including cancer and the poorly understood risks to the central nervous system constitute the major risks for exploration missions. Methods used to project risk in low Earth orbit (LEO) are viewed as highly uncertain for projecting risks on exploration missions because of the limited radiobiology data available for estimating risks from HZE ions. For the first-time we make a quantitative assessment of the uncertainties in cancer risk projections for space radiation exposures. Cancer risk projections are described as a product of many biological and physical factors, each of which has a differential range of uncertainty due to lack of data and knowledge. We use Monte-Carlo sampling from subjective error distributions that represent the lack of knowledge in each factor to quantify the overall uncertainty in risk projections. Cancer risk analysis is applied to several exploration mission scenarios including lunar station, deep space outpost, and Mars missions of duration of 360, 660, and 1000 days. At solar minimum, the number of days in space where career risk less than the limiting 3% excess cancer mortality can be assured at a 95% confidence level is found to be only of the order of 100 days. The current uncertainties would only allow a confidence level of less than 50% for a 1000-day class Mars mission, this is considered insufficient for assuring crew radiation safety at this time. A further result of this analysis is the quantification of the dominant role of biological factors in comparison to physical factors in the overall uncertainties for cancer risk projections. Approaches to reduce these uncertainties and mitigate risks that will enable the human exploration of space are discussed.

Table of Contents

List of Tables

List of Figures

1. INTRODUCTION

The human exploration of Mars is inevitable and will occur in the first-half of the 21st century. In planning these missions NASA will place a high priority on the health and safety of astronauts. A major area of concern is the possible detrimental effects on health, including cancer and other late effects such as cataracts, hereditary effects, and neurological disorders, caused by exposure to galactic cosmic rays (GCR) and solar particle events (SPE). The GCR contain highly ionizing heavy ions that have large penetration power in shielding and tissue and are unlike any radiation to which humans are exposed on Earth. Both the GCR and the SPE also contain significant numbers of high-energy protons, capable of large penetration and important nuclear interactions. A small fraction of SPE may produce extremely large doses leading to early radiation sickness or death if adequate shelter is not provided. Improved risk prediction and mitigation of radiation risks is essential to achieve exploration goals. For terrestrial radiation exposures, epidemiological data from the atomic-bomb survivors (Pierce *et al.*, 1996) and studies of other exposed cohorts (Cardis *et al.*, 1995) are used as a basis for risk prediction, however, there is no unambiguous approach for extrapolating human data from high dose-rate gamma ray exposures to the low dose-rate exposures of protons, heavy ions and secondary radiation in space. The National Academy of Science (NAS) and the National Council of Radiation Protection and Measurements (NCRP) have recommended postponing the definition of exposure limits for exploration missions until further information on the late effects of heavy ions is obtained (NAS, 1997; NCRP, 2000).

The NASA approach to radiation exposure in space is based on predicting the risk (probability of both short-term and long-term health effects). The determination of what constitutes an acceptable, i.e., "safe" risk level is and will remain a matter for continued attention. Setting radiation limits requires consideration of mission performance requirements without deviating from the highest ethical standards. An upper bound on levels of acceptable radiation risks for space exploration has not been determined and could be set higher than that of low Earth orbit (LEO) because of the nature of such missions (NAS, 1967).

The design of a mission to a given risk limit uses the predicted radiation environment as input for calculating possible radiation effects. However, mission safety can only be predicted within a defined confidence level, corresponding to the statistical nature of such a calculation. Mission design studies include cost versus benefit analyses of approaches to improve crew safety with higher confidence. Such studies are based on estimates of the uncertainties in such projections. The uncertainties at this time are large, and reducing them is one of the primary objectives of the NASA Space Radiation Health Research Program (Anon, 1998). This places even greater importance in having a realistic estimate of the uncertainty in the predicted risks since too large an estimate of uncertainty will result in excessive costs, while too small an estimate of uncertainty will result in excessive risk.

In this report we make a quantitative estimate of the uncertainties in the projection of lifetime cancer mortality for exploration class missions and discuss approaches to lower uncertainties and mitigate risks. Projecting the risk of late neurological disorders carries an even higher uncertainty than that of cancer mortality and is beyond the scope of this paper. Other risks to be faced by astronauts, while possibly substantial, can be addressed individually. The risk of hereditary effects is expected to be small, can be managed through counseling, and can be reduced through operational and shielding methods (NCRP, 2000). The risk of cataracts is known to be substantial following heavy ion exposures (NCRP, 2000), however it is not expected to occur during a mission and can be corrected by surgery if the onset of severe cataracts accelerated by exposure to space radiation. The risk of early health effects following a solar particle event can be effectively reduced to an acceptable level by the proper use of operational warning and dosimetry systems along with an adequate storm shelter for crew protection (Wilson *et al.*, 1999). However, because of their higher energies the cancer risk from GCR cannot be eliminated using operational approaches and practical amounts of radiation shielding. In fact, the use of high atomic mass shielding such as aluminum may increase risk, and lower mass materials provide a limited amount of attenuation (Wilson *et al.,* 1995; Cucinotta *et al.,* 2000a). It is important to quantify the possible range of cancer risks prior to mission design and to consider other approaches to reduce risk including biological countermeasures. We consider several mission types, including a lunar base, a deep space outpost and Mars exploration missions of various

lengths. A main conclusion of this report is that the uncertainties in cancer risk projections vary over a range of 4-6, substantially less than those noted by the National Academy of Sciences in 1997 (NAS, 1997). However, these large uncertainties severely limit a possible correlation between dose reduction and risk reduction at this time. We consider several approaches for risk reduction in this paper including operations, shielding, and biological countermeasures. Because of the small population sizes of astronauts, verifying the efficacy of most countermeasures will be difficult and truly revolutionary approaches will be needed.

2. ACCEPTABLE LEVELS OF RISKS

2.1 HISTORICAL PERSPECTIVE

In considering risk limitation for exploration class missions it is useful to consider historical recommendations that NASA has received from external advisory committees. Early radiation effects usually are related to a significant fraction of cell loss, exceeding the threshold for impairment of function in a tissue. These are "deterministic" effects, so called because the statistical fluctuations in the number of affected cells are very small compared to the number of cells required to reach the threshold (ICRP, 1991). Maintaining dose limits can ensure that no early effects occur, these are expected to be accurately understood (however, see Todd *et al.,* 1999). Late effects can be the result of changes in a very small number of cells, so that statistical fluctuations can be large and some level of risk is incurred even at low doses. Referring to them as "stochastic" recognizes the predominance of statistical effects in the manifestation of such effects.

Recommendations by NAS in 1967 (NAS, 1967) noted that radiation protection in manned space flight is philosophically distinct from protection practices of terrestrial workers because of the high-risk nature of space missions. The report of the NAS-1967 did not recommend "permissible doses" for space operations noting the possibility that such limits may place the mission in jeopardy and instead made estimates of what the likely effects would be for a given dose of radiation. In 1970, the NAS Space Science Board in response to a request from NASA made recommendations of guidelines for career doses to be used by

NASA for long-term mission design and manned operations. At that time, NASA employed only male astronauts and the typical age of astronauts was 30-40 years. A "primary reference risk" was proposed equal to the natural probability of cancer over a period of 20-years following the radiation exposure (using the period from 35 to 55 years of age) and was essentially a doubling dose. The NAS panel noted that their recommendations were not risk limits, but rather a reference risk and that higher risk could be considered for planetary missions or a lower level of risk for a possible space station (NAS, 1970). Ancillary reference risks were described to consider monthly, annual, and career exposure patterns. At the time of that report, the major risk from radiation was believed to be leukemia. By the end of the 1970's it was apparent that the risk of solid tumors following radiation exposure occurs with a much higher probability than leukemia's although with a longer average latency period before expression.

In the early 1980s several major changes had occurred leading to the need for a new approach to define acceptable levels of radiation risks in space. First, the maturation of the data from the Japanese atomic bomb (AB) survivors led to estimates of higher levels of cancer risk for a given dose of radiation. Second, the makeup of the astronaut population was changing with a much larger number of astronauts including mission specialists, the addition of female astronauts, and career astronauts of higher ages that often participate in several missions. In 1989, the National Council on Radiation Protection and Measurements (NCRP) issued their Report No. 98 that recommended age and gender dependent career dose limits using as a common risk limit of a 3% increase in cancer mortality above the background of average cancer mortality in the US population. The dose limits recommended by the NCRP correspond to average career duration of 10-years with the doses assumed to spread evenly over a career. The limiting level of 3% excess cancer fatality risk was chosen by comparing rates of occupational death in the "less safe" industries. The average years of life loss from radiation induced cancer death (about 15 years) is less than that of other occupational deaths. The use of cancer fatality instead of cancer incidence as a measure of risk limitation occurred for several reasons. Historical career dose limits referred largely to leukemia risk, which had a poor prognosis for cure until the 1980s, and therefore incidence and fatality were approximately the same. Fatality is also a more useful measure when comparing to other

occupational deaths since a large range of responses and suffering occurs for individual cancer types. Also, estimates of cancer risk must rely on the accuracy of record collection in exposed groups. In some aspects, but not all, the collection of records related to cause of death is more accurate than collection of records on cancer incidence, especially when the totality of all types is considered (NCRP, 1997). Finally, it should be noted that continued improvements in cancer treatments and prevention may affect how risk is limited in the future.

Organ	30 day limit (Gy-Eq)	1 Year Limit (Gy-Eq)
Eye	1.0	2.0
Skin	1.5	3.0
BFO	0.25	0.5

Table 1: Short-term absorbed dose limits (in Gy-Eq.) for preventing deterministic radiation effects for space activities in low Earth orbit (LEO) [data from NCRP, 2000].

	NCRP Report No. 98 (Sv)		NCRP Report No. 132 (Sv)	
Age, yr	Male	Female	Male	Female
25	1.5	1.0	0.7	0.4
35	2.5	1.75	0.9	0.6
45	3.25	2.5	1.5	0.9
55	4.0	3.0	2.9	1.6

Table 2: Career dose limits (in Sv) corresponding to 3% excess cancer mortality for 10-year careers as a function of age and sex as recommended by the National Council on Radiation Protection and Measurements [data from NCRP, 1989 and NCRP, 2000].

In the 1990s, the additional follow-up of the AB survivor data combined with a re-evaluation of the doses received by the survivors has led to further reductions in the estimated cancer risk for a given dose of radiation. New recommendations from the NCRP (NCRP, 2000), while keeping the basic philosophy of risk limitation in their earlier report, advocate

significantly lower doses limits than those recommended in 1989 (NCRP, 1989). Table 1 shows the current recommendations of short-term dose limits made by the NCRP in their report NCRP Report No.132 (NCRP, 2000). The recommendation to express the limits in terms of a dose modified by a relative biological effectiveness (RBE) factor for a given deterministic effect, rather than in terms of dose equivalent (or effective dose) takes account of the fact that quality factors used for conversion of absorbed dose into dose equivalent are intended as estimates of the relative effectiveness for carcinogenesis, rather than for deterministic short-term effects. Table 2 lists the long-term radiation limits recommended by the NCRP (NCRP, 1989; and NCRP, 2000). Both of these reports specify that these limits do not apply to exploration missions because of the large uncertainties in predicting the risks of late effects from heavy ions.

In comparison to NASA limits for LEO operations, the US nuclear industry has adopted age-specific limits that neglect any gender dependence. Here career limits are set at a total dose equivalent equal to the individuals Age $\times$ 0.01 Sv. Annual dose limits of 50 mSv (5 rem) are followed by US terrestrial radiation workers and help control the accumulation of career doses. NASA's short-term LEO dose limits are several times higher than that of terrestrial workers. Consistent with the ALARA principle, terrestrial workers and astronauts have been able to work long careers without approaching their respective dose limits. Exposures received by radiation workers rarely approach dose limits with the average annual exposure of 2 mSv which is a factor of 25 below the annual exposure limit. Similarly, transcontinental pilots, although not characterized as radiation workers in the US, receive annual exposures of 1 to 5 mSv and enjoy long careers without approaching exposure limits recommended for terrestrial workers in the US. The implementation of administrative dose limits, several times lower than legal limits, are common practice for terrestrial workers and are being implemented by NASA for astronauts in LEO (Williams and Cucinotta, 2000)[*].

[*] Williams, D.R., and Cucinotta, F.A., Integrated Space Radiation Protection Plan: Briefing to NASA Administrator, October 2000.

2.2 RADIATION QUALITY ISSUES

The GCR as they traverse though matter represents the most complicated radiation field that exists in nature. **Figure-1a** shows the fractional contribution from different elements to the fluence, dose, and dose equivalent. **Figure-1b** shows the energy distribution of particles in free space. A risk assessment model must be able to describe the biological action of each component of these distributions.

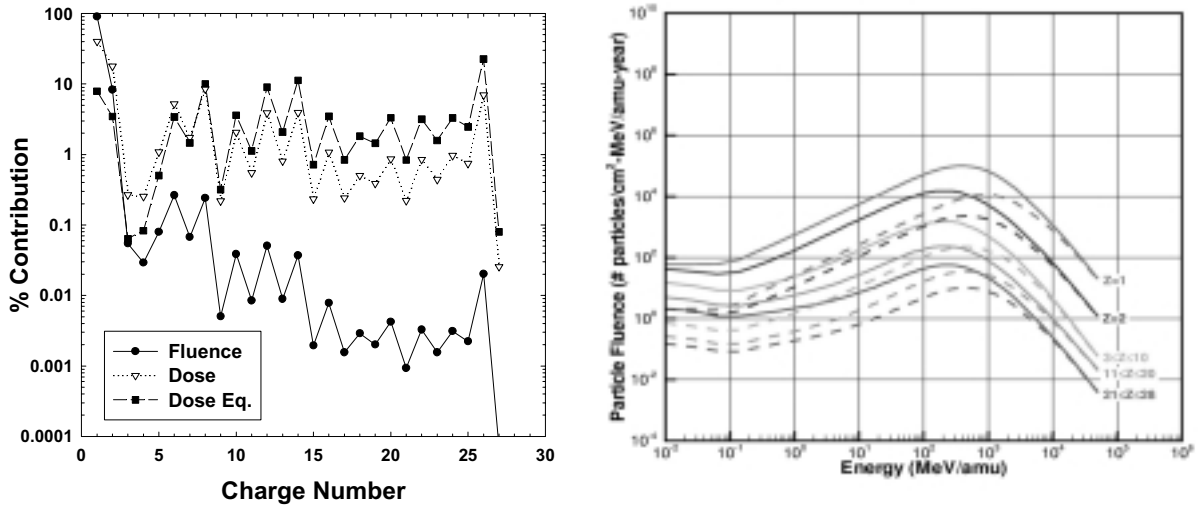

Figure 1: Percent contributions from individual GCR elements for the particle flux, dose, and dose equivalent at solar minimum (left plot, Figure-1a). The energy distribution of primary GCR particles with solid lines at solar minimum and dashed lines at solar maximum (right plot, Figure-1b).

The absorbed dose, D, of radiation represents the amount of energy deposited in bulk material and is expressed in units of joules per kilogram (J/kg), which is given the special name, Gray (Gy). For particle radiation, the absorbed dose is expressed as the product of the fluence of particles (the number of particles per unit area), F and the linear energy transfer (LET), L as

$$D = FL \tag{1}$$

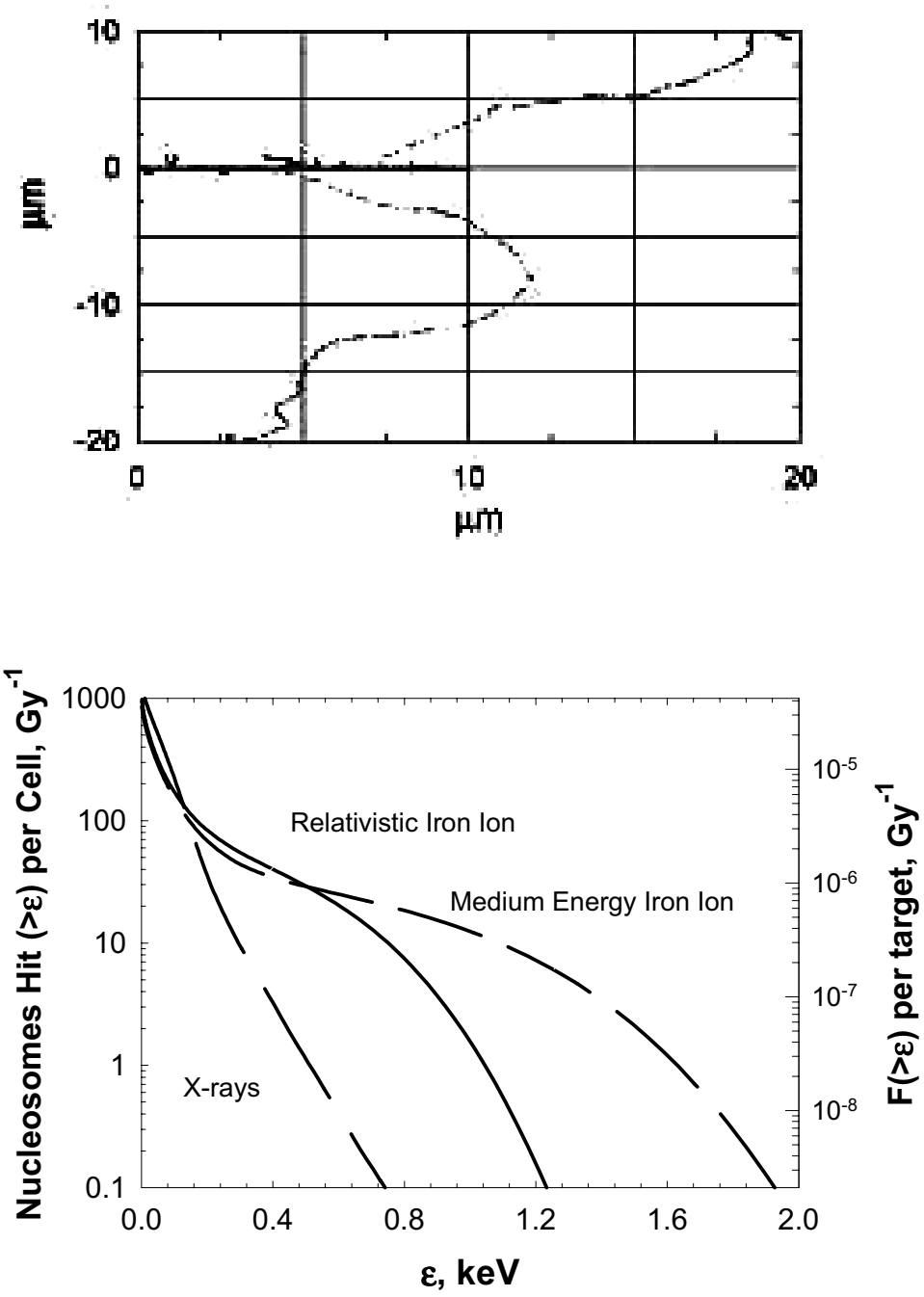

Figure 2: The spatial distribution of ionization events for a 1GeV/u iron particle is shown in the top plot (Figure-2a) [Nikjoo *et.al.,* 2001]. The spectrum of total energy deposition in a DNA nucleosome for x-rays and iron particles is shown in the bottom plot (Figure-2b) [Cucinotta *et al.,* 2000b].

The patterns of energy deposition occurring at the cellular or sub-cellular level are not described by LET; it merely describes the average rate of energy loss of a particle as it traverses matter. The absorbed dose is sufficient to characterize the magnitude of radiation consisting of a single component. For exposures with diverse radiation components, dose is of limited value because it does not provide a description of biological effects for different types of radiation. **Figure-2a** shows the spatial distribution of ionization events for a 1GeV/u iron particle in tissue (Nikjoo *et al.,* 2001). A large density region is formed about the trajectory of the track due to primary ionizations and low-energy electrons. High-energy electrons (ŭ-rays) traverse many microns away from the track. Table 3, which shows the average microscopic doses denoted as mean specific energy in several DNA structures for several radiation types. The large microscopic doses that occur for smaller structures are due to their small mass. In addition, **Figure-2b** shows the spectrum of energy deposition events in a DNA nucleosome (160 base-pairs in a 10x5 nm cylinder) for x-rays and iron particles (Cucinotta *et al.,* 2000b). There are energy deposition events in biomolecules that are not possible with low-LET radiation that do occur for high-LET radiation. Biophysical models show that differential radiation lesions are produced by such energy deposition events including complex DNA breaks and that there are qualitative differences between high-LET and low-LET radiation (Goodhead, 1994).

The approach used for estimating risks among humans exposed to nuclear particles is to consider experimental models to estimate relative effectiveness factors between ions and gamma rays (NCRP, 1993). These models are coupled with human data for gamma ray exposures to predict risks in humans for ions. The relative biological effectiveness (RBE), defined as the ratio of the dose of a reference radiation (usually assumed as x-rays or gamma rays) to the radiation under study that will produce an equal level of effect (for a given experimental observation), is the relative factor used most often and defined as:

$$RBE = \left(\frac{D_{x-ray}}{D_{ion}} \right) \tag{2}$$

Values of RBE extending over more than two orders of magnitude have been measured using cell culture and animal models. They are dependent on the biological end-point, cell, tissue, or animal type, dose and dose-rate, and the type of radiation (NCRP, 1993). Another limitation of the RBE approach is that the RBEs are usually not determined for many radiation types and at the dose-rates of interest for space radiation protection. The diversity of particle types that occur in space requires a large number of measurements to understand a detailed RBE relationship. The assumption of linearity of response at low dose-rates is a source of uncertainty since fluence rates in space can lead to more than one particle track per cell. If a threshold or quasi-threshold occurs at low doses of the reference radiation, RBEs that approach infinity are possible for high-LET radiation, however the effects of high-LET radiation may or may not be small when this occurs. Finally, it is possible that high-LET radiation produces effects that are qualitatively different from photons and therefore could not in principle be related to an equivalent dose of photons. Qualitative differences have already been established for the initial physical data and in some cases DNA or chromosome damage at low doses. However, the role of such effects in cancer formation is poorly understood.

		Mean Specific Energy z_D, Gy			
Particle Type	LET (keV/μm)	DNA Segment (2x2 nm)	Nucleosome (10 x 5 nm)	Chromatin Fiber (25 x 25 nm)	Cell Nucleus (100 μm^2)
X-rays	--	1.3×10^6	4.4×10^4	2.6×10^3	0.001
1 MeV proton	25.8	1.58	8.2	8.3	0.048
4 MeV proton	8.8	1.30	5.6	4.5	0.017
200 MeV proton	0.45	1.1	3.3	1.9	0.0008
1 MeV/u ^{4}He	103	2.26	16.8	24.0	0.19
5 MeV/u ^{4}He	32.2	1.48	7.7	6.9	0.06
5 MeV/u ^{12}C	278	2.57	21.8	30.6	0.50
200 MeV/u ^{12}C	16.3	1.24	5.3	4.3	0.029
5 MeV/u ^{56}Fe	3222	11.1	80.0	70.2	5.8
200MeV/u ^{56}Fe	303	2.72	23.7	30.4	0.55
600 MeV/u ^{56}Fe	173	2.08×10^6	15.2×10^4	18.4×10^3	0.31

Table 3: Dependence of the mean-specific energy for several cellular targets on radiation type [Cucinotta *et al.*, 2000a].

There is information from animal studies comparing tumor induction after neutron and gamma rays that suggests that neutron induced tumors are more aggressive appearing at earlier times. How such phenotypes originate at the molecular level has not been studied. For these and other reasons there are important limitations expected in using a RBE approach for risk assessment in space, however a practical alternative has not been accepted at this time. For neutron irradiation a large number of life-span studies with animal models have been performed and have formed the basis for risk estimation in humans following neutron exposures (Ainsworth 1982; Broerse *et al.*, 1993; Fry and Storer, 1987; Ullrich, 1984). DOE and NIH supported a small number of studies with heavy ion beams, in order to understand the risks to cancer therapy patients treated at the Lawrence Berkeley Laboratories, BEVALAC in the 1980s. No cancer incidence studies of either solid cancers or leukemia with heavy ion beams have received primary funding support from NASA. Such data will be needed for both the traditional approach to high-LET risk assessment and to support new molecular and genetics approaches.

National and international radiation protection policy committees make recommendations on values of RBEs to be used for assessing risks to humans. The approach taken by these committees have been to introduce a radiation quality factor (Q) or radiation weighting factor (w_R) that represents knowledge of RBEs and to determine the most appropriate RBE data to assign the dependence of Q on radiation type. The quality factors have been defined as a function of LET alone because there is lack of information to specify a more detailed relationship on particle type. Few occupational exposures to high-LET radiation occur and even then typically only neutrons and alpha emitters are of interest. Risk assessment for HZE particles is strictly a concern of NASA's and other space agencies. The increase in long-term missions in the future may lead NASA to institute its own policy of risk as a function of radiation quality for space radiation because of the important biophysical differences between HZE particles and terrestrial forms of radiation.

Tissue or Organ	Tissue Weighting Factor, w_T
Gonads	0.20
Bone Marrow (red)	0.12
Colon	0.12
Lung	0.12
Stomach	0.12
Bladder	0.05
Breast	0.05
Liver	0.05
Esophagus	0.05
Thyroid	0.05
Skin	0.01
Bone Surface	0.01
Remainder*	0.05

Table 4: Tissue Weighting Factors from ICRP (1991). Note: (*) For calculation purpose, the remainder is composed of the following additional tissues and organs: adrenals, brain, upper intestine, small intestine, kidney, muscle, pancreas, spleen, thymus, and uterus

The dose equivalent is defined as the product of the Q by the absorbed dose averaged over a specific tissue (D_T) or integrated over the LET distribution of the radiation field, $F(L)$,

$$H_T = D_T Q(L) = \int dL\, F(L)\, L\, Q(L) \tag{3}$$

The 'unit' of the dose equivalent is denoted as Sievert (Sv), and is not a true physical quantity. The concept of an effective dose (ICRP, 1991) has been introduced as a summation over radiation and tissue type using the tissue weighting factors, w_T,

$$E_T = \sum w_T H_T \tag{4}$$

	Male			Female		
Site	**ERR, Sv^{-1}**	**Back-ground**	**%ERR, Sv^{-1}**	**ERR, Sv^{-1}**	**Back-ground**	**%ERR, Sv^{-1}**
Stomach	0.15	9.7	1.5	0.65	5.5	3.6
Lung	0.33	5.0	1.6	0.75	2.5	1.9
Liver	0.52	3.7	1.9	0.11	1.6	0.2
Colon	0.57	1.3	0.7	1.08	1.1	1.2
Rectum	NA	1.0	NA	0.59	0.8	0.5
Pancreas	0.22	1.1	0.2	0.1	1.1	0.1
Esophagus	0.31	1.3	0.4	3.3	0.3	1.0
Gall bladder	0.9	0.8	0.6	0.41	1.0	0.4
Bladder	1.99	0.2	0.4	0.44	0.1	0.1
Uterus	-	-	-	0.23	2.6	0.6
Breast	-	-	-	0.79	1.1	0.9
Ovary	-	-	-	0.87	0.7	0.6
Prostate	0.44	0.6	0.3	-	-	-
Lymphoma	0.27	0.5	0.1	-0.17	0.6	
Myeloma	1.28	0.1	0.1	1.25	0.2	0.3
Other Solid	0.36	3.5	1.2	0.84	2.4	2.0
All Solid	0.375	0.28	0.28	0.774	0.2	0.14

Table 5: Site specific excess relative risks (ERR) for dose of 1 Sv for fatal cancer for males and females exposed at age 30 yr [data from Preston *et al*., 1996].

Values of the tissue weighting factors are given in Table 4. These are merely estimates of the average contribution from specific tissues to the overall cancer burden (ICRP, 1991). In actuality, tissue weighting factors would have a strong dependence on age and gender. Table 5 shows site specific excess relative risks (ERR) for 30 year olds (Pierce *et al.*, 1996) for different tissue types and their contributions can be seen to be distinct from those of Table 4. The distribution in tissue types provides an indication of cancer types that dominated risk to the atomic bomb survivors. In contrast, the tissue weighting factors are defined to reflect the total detriment from radiation exposure, which includes consideration of the years of life-loss expected for different types of cancer deaths, cancer morbidity and hereditary effects. The total risk for cancer is evaluated as

$$Risk = \Sigma_T R_{0T}\,(age, sex)\, H_T \qquad (5)$$

where, R_{0T} are the appropriate risk coefficients for incidence or mortality, respectively that are dependent on age at exposure, gender, and tissue type.

2.3 HISTORICAL EXPOSURES IN NASA PROGRAMS

In discussing cancer risks for exploration missions it will be useful to first review the radiation exposures astronauts have received in the past. The doses received by astronauts depend strongly on several factors including orbital inclination, altitude, period in the solar cycle, and mission duration. Radiation sources in LEO include contributions from trapped protons and electrons, galactic cosmic rays (GCR), and sporadic exposures from solar particle events. The energy spectrum of each source determines their range in shielding material and the human body. Trapped electron energies extend to a few MeV with ranges of 1-2 cm in water and include a small bremsstrahlung component capable of reaching larger depths. Trapped protons have energies extending to several hundred MeV, however more than 90% of the flux is from particles with ranges less than 1 cm in water. A small high-energy component is capable of penetrating crew compartments and tissues producing nuclear secondaries including neutrons and highly ionizing hydrogen, helium, and heavy ions (Cucinotta *et al.,* 2000a). In contrast to trapped radiation, incident GCR in LEO are dominated by relativistic particles with energies of 1 GeV/u or higher since the Earth's magnetic field provides shielding from the lower energy components. Relativistic ions have large ranges and undergo numerous nuclear reactions inside shielding and other materials (e.g. body tissues). Nuclear reactions can lead to a large build-up of secondary particles including neutrons, hydrogen and helium ions, heavy ions, and mesons, especially for materials with high atomic mass constituents. For the deep space Apollo missions, the GCR dominated organ doses with a small contribution from passage through the trapped belts. Low-energy trapped radiation dose is attenuated effectively by shielding. For galactic cosmic rays, very little or no attenuation of the dose or dose equivalent occurs because of the balance between particle loss and production processes and materials such as aluminum provide no radiation protection (Wilson *et al.*, 1995; Cucinotta *et al.*, 2000a).

Figure-3 shows the dose and estimated effective doses received by all astronauts over the course of NASA programs and Table 5 shows the average doses and dose-rates for specific mission types. These results use records of passive dosimetry worn on all NASA missions (excluding the first four Mercury missions where dosimetry was not utilized) through the end of 1999 and effective doses are estimated using area dosimetry and space radiation transport

codes (Cucinotta *et al.,* 2000a). Several features are prominent including the large increase in doses at higher altitudes due to longer sampling of the Earth's trapped radiation belts and the increase in average quality factors for high inclination and deep space missions. Average quality factors range from about 1.6 to 3.0 with the highest values occurring for GCR dominated mission. The comparison in Table 5 for 28.5^0 missions with altitudes above 400 km includes the Hubble telescope launching and the several Hubble service missions with altitudes near 600 km where the higher altitudes lead to large increases in trapped radiation. The International Space Station (ISS) is in a 51.6^0 inclination with altitudes that will range from about 360 to 450 km. Since ISS is basically an aluminum structure similar to past NASA vehicles in their shielding mass distributions, dose-rates to the BFO in the range from 0.4-1.1 mSv/day can be expected during the course of the solar cycle and considering local shielding variations.

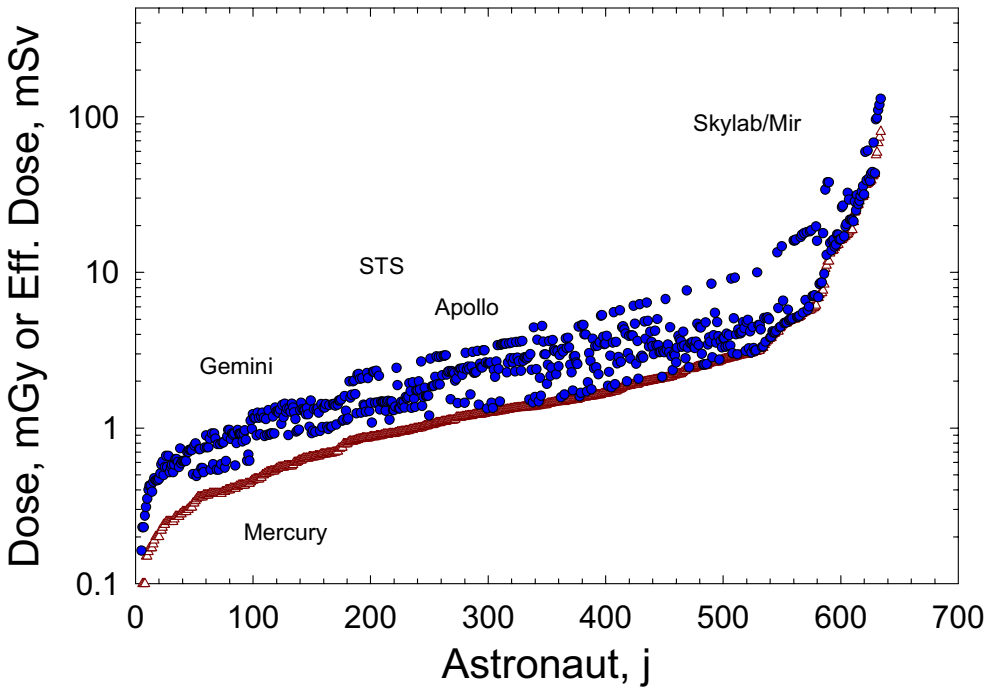

Figure 3: Historical radiation doses (triangles) as recorded on the personal dosimeter badges and estimates of the effective doses (circles) for astronauts from all NASA Missions (through December 1999).

NASA Program	Inclination (degrees)	Altitude (km)	Crew (number)	D (mGy)	H (mSv)	D-rate (mGy/d)	H-rate (mSv/d)
Mercury	--	--	6	0.1	0.15	0.3	0.55
Gemini	--	--	20	1.3	2.2	0.49	0.87
Apollo	--	--	33	4.1	12.0	0.43	1.2
Skylab	50	430	9	40.3	95.0	0.71	1.4
ASTP	50	220	3	1.1	2.3	0.12	0.26
STS	28.5	>400	85	9.5	17.0	1.2	2.1
STS	28.5	<400	207	0.9	1.6	0.1	0.18
STS	39-40	~400	57	1.1	2.4	0.1	0.21
STS	>50	>400	10	2.2	5.2	0.44	1.1
STS	>50	<400	190	1.7	3.8	0.2	0.45
NASA-Mir	51.6	~390	7	50.3	115	0.37	0.84

Table 6: Average dose (D) or dose-rate recorded by dosimetry badge and estimates of the dose equivalent (H) to the BFO received by crews in NASA programs through 1999.

Astronauts also receive exposures from diagnostic x-rays, experimental protocols and extensive air training. An historical summary of these exposures is provided in Table 7. The exposures from diagnostic x-rays decreased dramatically by the mid-1980s due to a Presidential Directive ordering improvements in procedures used by government agencies. Also, of note is that on the Apollo 12 through Apollo 17 missions a ^{238}Pu source was used for a lunar surface experiment (English and Liles, 1972) and led to a small neutron dose with higher doses occurring on the aborted Apollo 13 mission because the experiment was not delivered to the lunar surface. For air-travel, the listed values are preliminary estimates using the approximate number of hours of training required for pilots and mission specialists and the typical flight routes. Although, space radiation is the dominant component of collective doses, clearly other types of exposures make significant contributions for individual astronauts. Using the recent NCRP risk estimates (age and gender dependent), we can estimate that none of the NASA astronauts have reached a lifetime risk more than 1% excess cancer fatality. Astronauts selected for a Mars mission will have some non-negligible radiation exposure history (on the order of 0.5%) if they have participated in prior ISS or Space Shuttle missions and such prior exposures will be factored into the acceptable level of risks for exploration mission crews.

Radiation Source (collective)	Historical collective doses over time period-				
	1957-1969	**1970-1979**	**1980-1989**	**1990-1999**	**Total**
Space					
cSv-PY	20	111	42	273	**446**
(Average, cSv)	(0.46)	(4.0)	(0.26)	(0.73)	**(0.74)**
Radioactive source (Pu)					
cSv-PY	-	2.8	-	-	**2.8**
(Average, cSv)		(0.2)			**(0.2)**
Diagnostic (x-rays)					
cSv-PY	141	179	52	15	**387**
(Average, cSv)	(0.095)	(0.082)	(0.027)	(0.007)	**(0.05)**
Air-flight (training)					
cSv-PY	20	32	40	65	**157**
Total Collective					
cSv-PY	**181**	**324.8**	**134**	**353**	**992.8**

Table 7: Historical collective doses in person years (cSv-PY) and average occupational doses from individual sources amongst the NASA astronauts.

2.4 RADIATION AND CANCER RISKS

In considering projections of cancer risks of astronauts participating in exploration missions, it is useful to consider the expected normal burden of cancer risks in the general population. Cancer is a genetic disease and the incidence of cancer increases with a strong-age dependence as shown in **Figure-4**. The increase in incidence with age is related to the accumulation of genetic alterations from environmental or spontaneous mutations and processes denoted as genomic instability. Hereditary disorders in the germ line cells often lead to childhood cancers or increased risk in some adults. There have been many breakthroughs in recent years in discovering the molecular and genetic mechanisms leading to cancer (Vogelstein and Kinzler, 1997). This knowledge indicates that there are a large number of molecular pathways whose alteration is causative of carcinogenesis that are differential across and within specific tissues types. The DNA lesions and oxidative damage produced by radiation are non-specific and most likely act in many of these pathways. The

roles of cancer pre-disposition and DNA polymorphisms are expected to play an important role in an individual's risk of radiation-induced cancer.

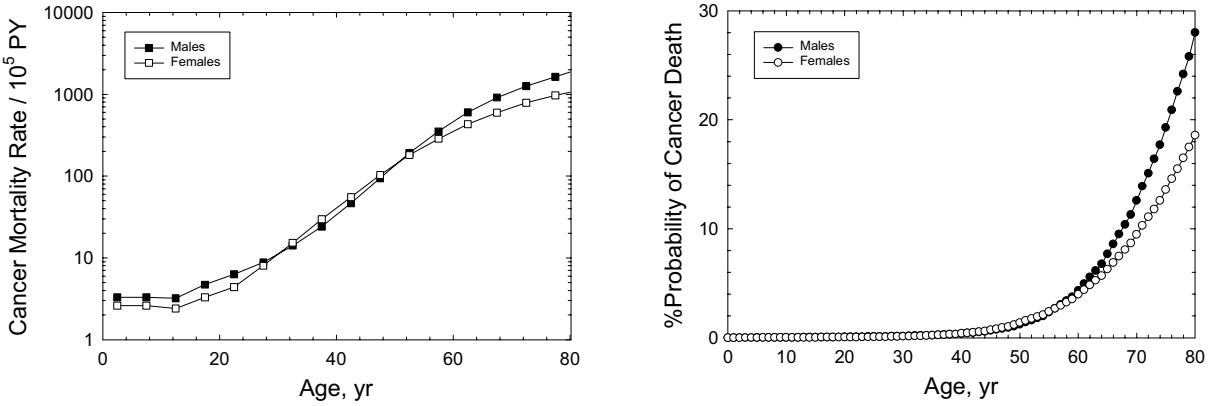

Figure 4: Cancer death rates in the US population (left) and probability of cancer death as a function of age (right) [data from SEER, 1999].

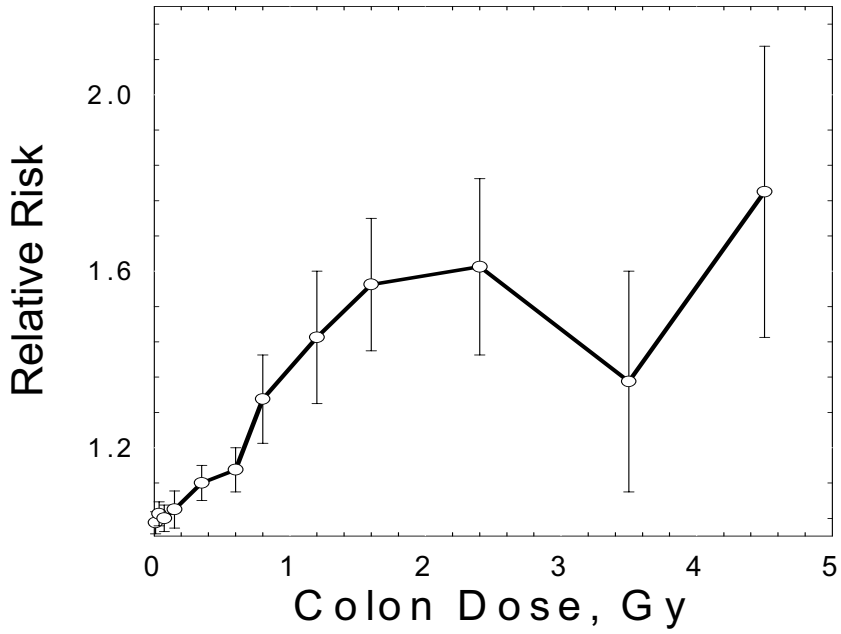

Figure 5: Relative risk versus dose for solid cancers in the atomic-bomb survivors [data from Pierce, *et al.,* 1996].

The major epidemiological data set for cancer risks following radiation exposure are from the survivors of the atomic-bomb explosions in Hiroshima and Nagasaki (Preston, 1994).

Figure-5 shows the relative risk for solid cancers as a function of dose for AB survivors. The dose response appears linear at low doses for solid cancer, and reaches a plateau prior to an apparent turn-down at higher doses from what are generally called cell sterilization effects.

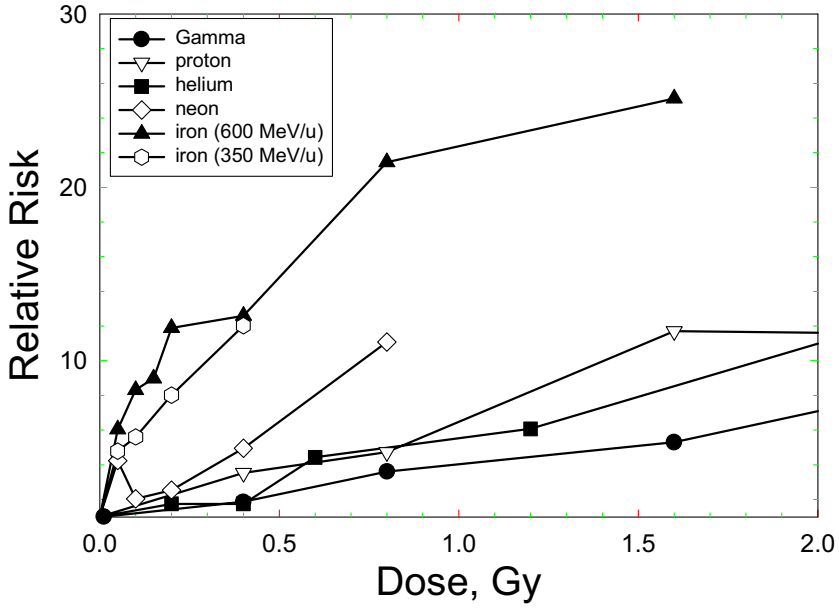

Figure 6: Relative risks for the prevalence at 600 days of Harderian gland tumors versus particle fluence [data from Alpen *et al*., 1993].

As a comparison to human data, **Figure-6** shows the dose-response data for Harderian gland tumors in the mouse for gamma rays and several heavy ions (Alpen *et al.*, 1993). Note, compared to the response to gamma rays, the response for heavy ions is much higher at low-doses and that a bending of the dose response occurs at a modest dose. The bending of the dose-response makes it difficult to verify an initial linear region with significant confidence. The much higher relative risks in the data of Alpen *et al.,* 1993, compared to the AB data is due to several reasons. However, the comparison is made here to illustrate the differences that do occur and the lack of data to make a proper judgment of risk.

The AB data can be grouped into several variables including gender, organ site and age at exposure and by age of cancer appearance or death. The grouping of data across all organs,

and into a lifetime risk decreases the uncertainty in risk estimates, however information is lost that is useful for estimating an important part of the detriment, the age of appearance of cancer. The use of pooled data eliminates possible considerations of differences in radiation quality on cancer type, latency, and average loss of life expectancy. Data in animals suggest that the later information is quite important because of the much earlier appearance of tumors following high-LET radiation compared to low-LET radiation (Fry and Storer, 1987).

Low-LET risk coefficients are obtained from fitted dose-response models of cancer incidence among the Japanese survivors (Preston *et al.*, 1994; Thompson *et al.*, 1994; Pierce *et al.*, 1996). The two statistical models used most frequently for fitting cancer incidence dose-response relationships are the additive and multiplicative Poisson regression models. Excess relative risk is obtained by fitting multiplicative models and is defined as the ratio of cumulative risk at a given age among the exposed to cumulative risk among the non-exposed. Absolute risk is obtained by fitting additive models and represents the difference between cumulative risk among the exposed and the non-exposed groups. Fitted risks are used for projecting cumulative risks among exposed populations.

The small population size of astronauts would make it extremely difficult to show any attribution of increased cancer risk to radiation. For example, the lifetime probability in the US for cancer death is currently 22% (SEER, 1999) such that a 3% excess fatal cancer risk corresponds to a relative risk (RR) of 1.14. Power analysis using birth dates for the 295 astronauts since the Mercury program show that a RR > 2.1 would currently be needed (estimated as RR > 2.0 in 2010), before an increased cancer risk could be detected at a 95% confidence level relative to the general population. Such a comparison would be limited further by other confounding factors including a possible healthy worker effect, the large number of national and demographic backgrounds of astronauts, and other possible carcinogens during space activities. An important factor would be the time of cancer appearance, especially for high-LET radiation. For long-term space flight (>30 days) a significant fraction of annual or career exposure will be incurred by astronauts and for some mission designs, exposure standards would be exceeded without an excessive cost for the addition of radiation shielding possibly leading to the cancellation of the mission due to the

large costs. Because, as the above discussion shows, any increase in cancer from radiation exposure would be extremely difficult to verify for a small population, highlights the importance of the accuracy of risk projections. The role of reducing uncertainties in risk assessment cannot be underestimated under these conditions.

3. EVALUATION OF UNCERTAINTIES

3.1 CANCER RISK ESTIMATES

Previous studies have concluded that the uncertainties in risk projections for exploration class missions are large and that new research and mitigation approaches are needed (NAS, 1970, 1973, 1997). The National Academy of Sciences (NAS, 1997) and the National Council on Radiation Protection and Measurements (NCRP, 2000) have made recommendations to NASA on vital data collection and research needs and approaches to reduce risk projection uncertainties. We now attempt to quantify the uncertainty in the cancer risk projections for exploration class missions using subjective confidence intervals to represent current knowledge of individual factors that contribute to risk projection and evaluate the propagation of errors through Monte-Carlo sampling techniques. The value of this approach is that when considering multiple factors that contribute to risk estimation, an overestimate or underestimate of the uncertainty can be made by assuming that the uncertainties are multiplicative. By applying these methods to actual scenarios for exploration class missions, the importance of individual factors in the overall uncertainty can be studied and methods to reduce uncertainties optimized.

For low-LET radiation, an increased fatal cancer probability of 4% for a low dose-rate exposure of 1 Sv (4.0×10^{-2} Sv^{-1}) is expected for the average adult worker. A recent error analysis of the risk projections for low linear energy transfer radiation by the National Council on Radiation Protection and Measurements (NCRP) estimated 90% subjective confidence intervals of 1.15×10^{-2} Sv^{-1} to 8.08×10^{-2} Sv^{-1} with a median value of 3.69×10^{-2} Sv^{-1} compared to the expected value of 4.0×10^{-2} Sv^{-1}. Since this analysis did not consider the contributions to the overall uncertainty due to radiation quality or the ability to determine the dose of radiation in space or on other planetary bodies, we can expect a much larger

uncertainty for exploration class missions. In Table 8, we list the expected implications of outcomes of confidence interval estimates relative to legal standards for risk limitation. Clearly, if a significant fraction of the confidence interval approaches or exceeds legal standards, efforts to reduce uncertainties in risk projections through research and data collection, and increased emphasis on risk mitigation planning are vital.

Risk Projection Relative to Legal Standard	Implications	Recommended NASA Actions
95th percentile > Legal standard & 50th percentile > Legal standards	Very likely that legal standards will be exceeded	Data collection and research are vital; revolutionary approaches to risk mitigation needed; mission may be unsafe or too high of cost for risk reduction
95th percentile > Legal standard & 50th percentile < Legal standards	Legal standards may be exceeded	Emphasize mitigation and perform further data collection and research to reduce risk uncertainties
95th percentile < Legal standard	Very unlikely that legal standards will be exceeded	Judge cost effectiveness of risk mitigation measures; research and data collection not vital

Table 8: Implications from projections of quantitative uncertainty levels relative to the legal standards.

3.2 METHODOLOGY

For projecting life-time cancer fatality risks, the accepted approach is to multiply an age and gender dependent risk coefficient by the radiation dose and the quality factor for each component that contributes to the exposure, and to assume additivity of effects of each component, *j*, as:

$$R(age, sex, Dose) = \sum_j R_0(age, sex) D_j(L) Q_j(L) \tag{6}$$

Equation (6) is a multiplicative model of risk, consisting of a product of several factors: the risk coefficient, R_0, the physical dose as a function of LET (L), and the assignment of the radiation quality factor to each component. As discussed next, the risk coefficient, R_0 is itself

a product of many factors. The limiting behavior of the addition of many random variables is well known as the normal distribution. In contrast, the limiting behavior of the multiplication of many random factors will be a log-normal distribution. In performing our analysis we will explicitly assume that each factor in equation (6) is independent. This assumption may not be strictly valid for exploration class missions because of the possibility of non-additivity of components since cells will be traversed by multiple particles and ŭ-rays produced by ions passing through adjacent cell layers (Cucinotta *et al.*, 1998a). Alternative approaches to risk estimation are discussed in an Appendix A.

3.3 Uncertainties in Low-LET Risks

The NCRP Report No.126 considered the overall uncertainty is the risk coefficient for the average adult worker, which we summarize next. The risk coefficient is written as:

$$R_0(age, sex) \quad = \quad r_0(age, sex)\left[\frac{x_D x_S x_T x_P x_U}{x_{Dr}}\right] \tag{7}$$

where, r_0 is the baseline risk coefficient and the x_α are quantities (random variables) whose values are sampled from an associated probability distribution functions (PDF), $P(x_\alpha)$ that represent the distribution in uncertainties for each factor that contributes to the risk estimate. The NCRP Report No.126 defined subjective probability distribution functions, $P(x_\alpha)$, for each factor that contributes to the low-LET-risk projection:

1. $P_{dosimetry}$ represents the random and systematic errors in the estimation of the doses received by individuals exposed to the Hiroshima and Nagasaki atomic-bomb blasts. NCRP Report No.126 considered the uncertainties due to the evaluation of kerma, random fluctuations, neutron dose and RBE. $P_{dosimertry}$ is assumed as a normally-distributed PDF for bias correction of random and systematic errors in the dosimetry (DS86) with mean 0.84 and standard deviation 0.11
2. $P_{statistical}$ represents the distribution in uncertainty in the risk coefficient r_0. This uncertainty will be dependent on the age and sex at the time of the exposure. It is

assumed as a normally distributed PDF with a mean of one and a standard deviation of 0.15

3. $P_{transfer}$ represents the uncertainty in the transfer of cancer risk following radiation exposure from the Japanese population to the US population. Both additive and relative risks models were considered by NCRP No.126 in assessing the uncertainties in such transfer. $P_{transfer}$ is log-normal with mean 1 and standard deviation 0.26 (GSD=1.3)
4. $P_{projection}$ is the PDF for bias correction of uncertainty in projection of cancer risks over a lifetime. It is assumed as triangle distribution with a 90% confidence limits 0.62 and 1.05 with a peak at 1, i.e., triangle (0.62,1,1.05)
5. P_{U} is the normally-distributed PDF for a bias correction of unknown uncertainty that has mean 1 and standard deviation 0.3
6. P_{Dr} represents the uncertainty in the knowledge of the extrapolation of risks to low dose and dose-rates (DDREF). For exploration missions, data at comparable doses is available in humans and experimental models and the dose-rate reduction is an important uncertainty. The P_{Dr} is assumed to be a truncated triangle distribution starting at 1 and ending at 5 with a peak at 2

Since we consider age and gender specific risk coefficients, the actual statistical uncertainty will be somewhat larger than assumed in NCRP Report No.126 since a smaller number of persons and cases will contribute to age and sex specific tallies of cancers than does the risk coefficient estimated for an average adult worker. However, since this uncertainty will be smaller than the others considered in the present analysis they are neglected. Methods to treat age and gender dependent risk for cancer incidence are described by Peterson and Cucinotta (1999).

In performing the Monte-Carlo sampling, each of the variables, x_α is defined over an interval as determined by the domain of the associated PDF. A random number is selected for each variable in a manner that is consistent with the associated PDF and the corresponding value of x_α is determined. This sampling process is repeated a large number of times until a convergent distribution obtained. The largest contributor to the distribution in uncertainty for

low-LET radiation is the dose and dose-rate reduction factor (DDREF) (NCRP, 1997) comprising about 40% of the uncertainty. Future prospects for reducing the low-LET uncertainty are discussed below.

3.4 Uncertainty in High-LET Risks

In order to estimate the uncertainty in the risk from high-LET radiation, we consider the uncertainty in the specification of the radiation quality factor by folding the low-LET risk uncertainty model (described above) with a probability density function for the quality factor, *P(Q(L)),*

$$R(age, sex, Dose) \quad = \quad R_0(age, sex) D(L) Q(L) x_Q \tag{8}$$

To form a basis for the functional form of $P_Q(x_Q)$, we first consider past reviews on the relative biological effectiveness of high-LET radiation. These include the ICRP Report 60 (1991), ICRU Report 40 (1986), and NCRP Report 104 (1990) as well as recommendations to NASA in the reports cited above by NAS or NCRP. The philosophy for assigning radiation quality factors followed by these committees is to consider an average of RBEs at low doses (RBE_{max}) for the most relevant experimental endpoints and to assume the linear-additivity model holds.

Endpoint	**RBE_{max}**
Tumor induction	~3-200
Life Shortening	15-45
Transformation	35-70
Cytogenetic studies	40-50
Genetic endpoints in mammalian systems	10-45

Table 9: RBE_{max} for fission (or optimal energy) neutrons vs. gamma rays for stochastic endpoints [data from ICRU, 1986].

The most well studied high-LET radiation has been fission neutrons where a large number of studies including tumor induction and life-shortening in animals, and cellular transformation, mutation, and cytogenetics have been performed. Table 9 shows a summary of RBE_{max} for fission neutrons from ICRU Report No.40. DOE and NIH supported many studies on the biological effectiveness of neutrons in the 1970s and 1980s forming a basis for RBE estimates for neutrons. However, we note that the neutron weighting factors are not the most conservative values that could be inferred from such data. Rather, it has been argued that the maximum RBE values for life-shortening in mice are the most appropriate values (Storer and Mitchell, 1984). However, these values differ among strains of mice. Also, RBEs for lethal and non-lethal tumors in rats are often above values of 50 (Wolf *et al.*, 2000) indicating that higher RBEs perhaps occur in rats than mice leaving the situation for humans uncertain.

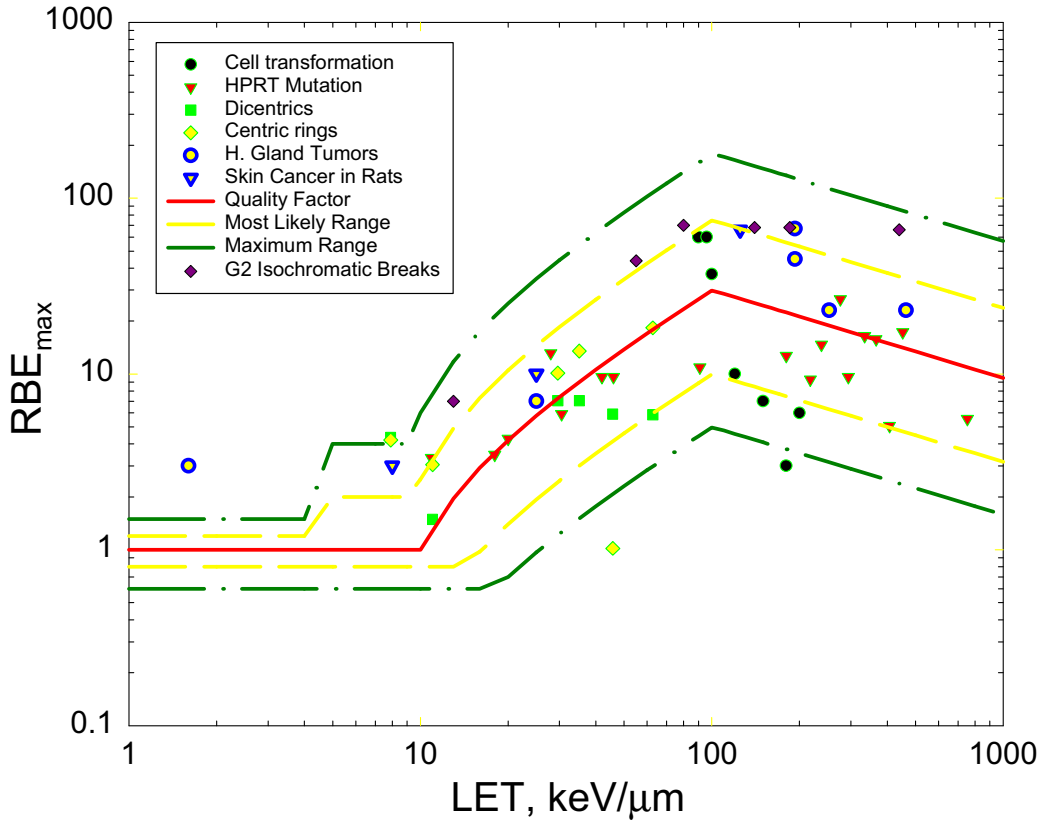

Figure 7: Ranges of RBE values observed in experimental models as a function of LET are shown along with the *Q(L)* relationship (solid line). For defining a PDF for the uncertainty in *Q(L)*, in the inner region bounded between the lines (dash) a uniform probability is assumed. In the outer region bounded between the lines (dash-dot) a lower probability is assumed.

In contrast to the many neutron studies, due to the lack of a facility to simulate space radiation on the ground, there is only a limited number of data available for HZE particles. The major studies are summarized in **Figure-7.** Also, shown in **Figure-7** are the current radiation quality factors (ICRP, 1990). Clearly, these values are not conservative for HZE ions and in almost all cases data for HZE induced cancers in animals (the most relevant endpoint) are under estimated by the quality factor, Q. In several cases direct comparisons between fission neutrons and HZE particles can be made. Experiments studying the transformation of Syrian hamster embryo (SHE) cells showed a high effectiveness for 500 MeV/u Argon ions similar to neutrons of an energy (0.46 MeV) corresponding to the peak in neutron biological effectiveness (Borek *et al.,* 1978). The experiments of Fry *et al.* (1983) and Alpen *et al.* (1993) for tumor induction in the mouse Harderian gland showed a high induction rate with iron particles and also that iron particles where less effected when promotion was enhanced using pituitary isografts than other radiation types including fission neutrons and gamma rays. Included in **Figure-7** is the large RBE for fractionated exposures to Fe particles which indicate a 50% increase in tumor rate compared to an acute exposure for a dose of 40 cGy (Alpen *et al.,* 1993; Edwards, 2001). In contrast, in a study of life-shortening, Ainsworth *et al.* (1986) has observed that fission neutrons where more effective than several heavy ions tested.

Studies of skin cancer induction in rats with heavy ion beams have shown extremely high values of RBE (>100). However, the high values of RBE may be related more to the ineffectiveness of low-LET radiation at low doses (Burns *et al.,* 1994) than the high effectiveness of heavy ions. In **Figure-7** we include RBEs for skin cancer (Burns *et al.,* 1994) estimated for a moderate dose of electrons, and note that initial slope estimates would be much higher. For the induction of cataracts in rats, extremely large RBEs (>200) are observed with both low energy neutrons (NCRP, 1989) and HZE ions (Worgul *et al.*, 1992). There is no basis to believe that many HZE ions are less effective than neutrons. Rabin and Joseph (2000) have observed late deterministic effects in the CNS of the rat that occur at low doses of Fe particle, and are not observed following low doses of x-rays or fission neutrons indicating a large RBE. For cytogenetic endpoints, large RBEs are observed by Sasaki *et al.,* (1998) and Kawata *et al.,* (2000). It was shown that iron ions have RBEs > 80 for initial G2

chromatid breaks and the fraction of remaining G2 breaks after several hours of rejoining. One limitation with the studies noted above is that only a few particle charges and energies were considered and it is possible that other HZE ions are more effective than the ones tested. The need for biophysical models (Katz, *et al.,* 1971 and Cucinotta *et al.,* 1999a) to extrapolate data limited to only a few ion types is vital for GCR risk assessment.

Values of RBE for high-energy protons (E>10 MeV) have been in the range from 0.6-2.0 with the higher values observed at energies above a few hundred MeV (NCRP, 2000). The increase at higher energies is attributed to the effects of target fragmentation and can be treated in an additive manner consistent with equation (5) (Cucinotta *et al.*, 1991). Few studies of proton effects have been made at low doses or dose-rates, leaving some possibility that part of the increase in RBE above unity are not entirely from nuclear secondaries. Biophysical considerations suggest that these possibilities are not likely.

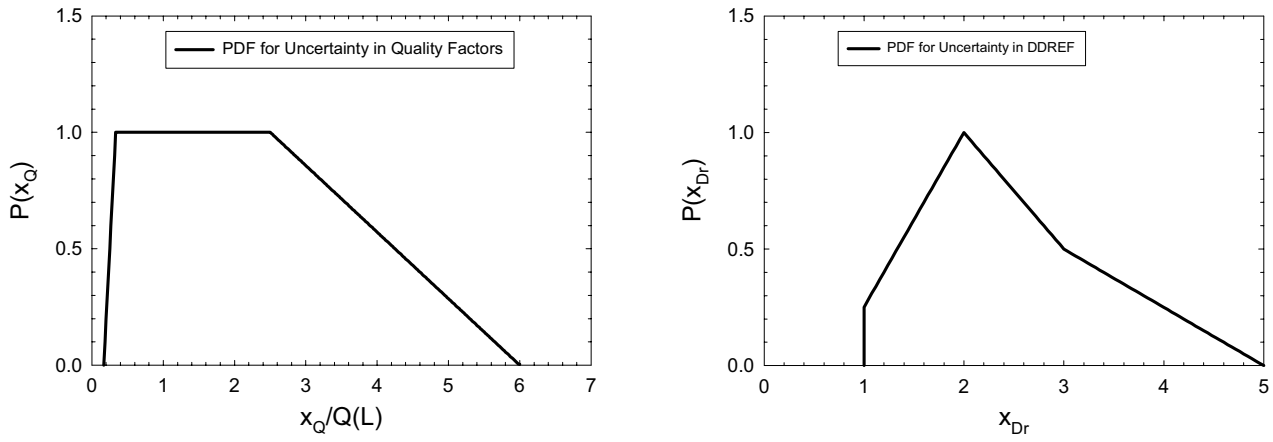

Figure 8: Probability Distribution Function (PDF) for uncertainty in quality factor, Q (left plot, Fig.8a) and the PDF for uncertainty in DDREF (right plot, Fig.8b) [data from NCRP 126, 1997].

Based on these observations there is no basis to expect that the current quality factors are accurate to within a few times above or below their nominal values for ions of medium and high values of LET. Of course, differences in RBEs for specific tumor types or perhaps individuals may occur and cannot be estimated at this time. We thus represent the PDF for the uncertainty in the *Q(L)* using a uniform distribution over the range $Q/3 < x_Q < 2.5\ Q$ and

assume a linearly decreasing probability at higher and lower values with a zero probability below *Q/6* and above *6Q*. For LET< 10 keV/μm these values are adjusted to 0.8 to 1.5 for the uniform region and 0.6 and 2 for the upper and lower bounds, respectively. This PDF is illustrated in the left hand panel of **Figure-8.** The upper limit of 6 times the quality factor corresponds to a value of about 180 and is within the range of experimental observations for late effects. In the right hand panel of **Figure-8,** we show the PDF for the DDREF.

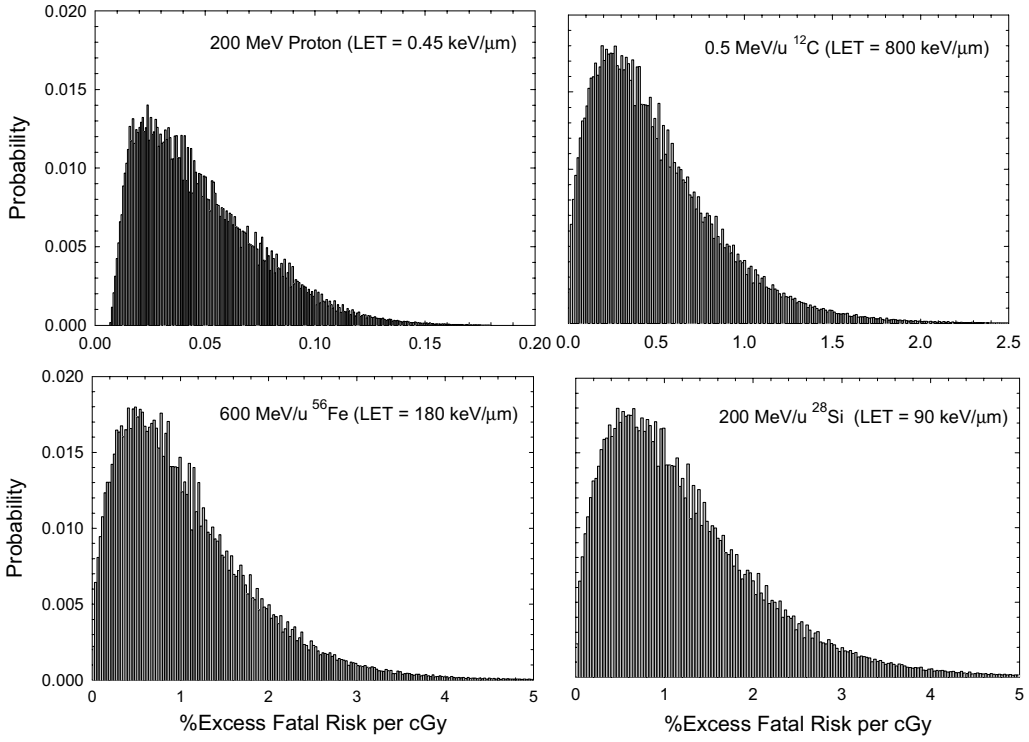

Figure 9: Uncertainty distribution for lifetime excess fatal cancer risk for a 1 cGy-dose of 200 MeV protons (LET=0.45 keV/μm), 0.5 MeV/u of carbon (LET=800 keV/μm), 600 MeV/u of iron (LET=180 keV/μm), or 200 MeV/u of silicon (LET=90 keV/μm)

Figure-9 shows examples of histories for the distribution of biological risk for several HZE ions normalized to a dose of 1 rad (10 mGy). The ordinate plots the values of risk, and the abscissa the probability that this value of risk occurs. **Figure-10** shows the risk per rad (cGy)

and standard errors as a function of LET that results from the Monte-Carlo sampling. We used 20,000 trials per LET value in our analysis.

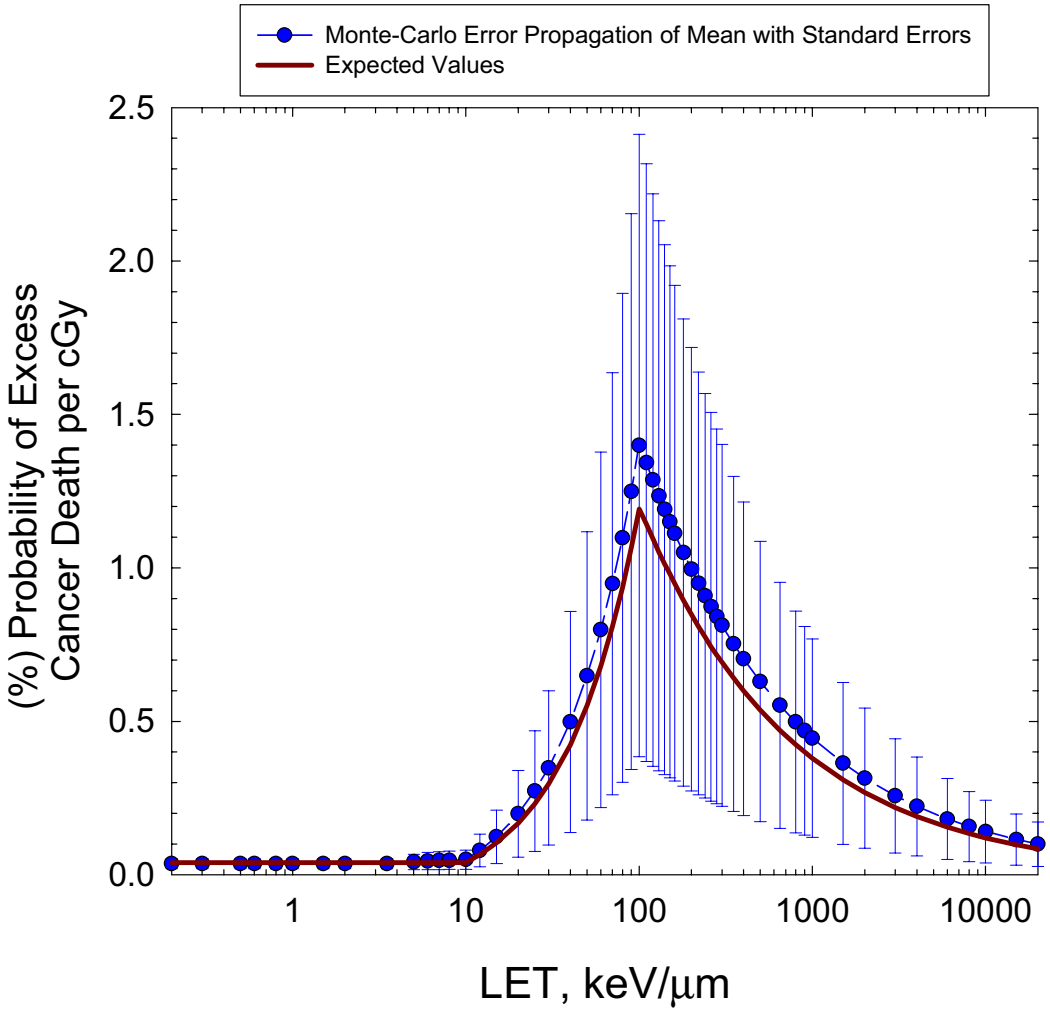

Figure 10: Calculated expected and mean values of the probability of excess fatal cancer per cGy as a function of LET with standard errors.

3.5 Uncertainties in Physical Variables

The uncertainties in physical factors occur in three areas: the knowledge of the GCR composition and energy spectra, the description of the physical transport processes of particle through materials and tissues, and the knowledge of the amount of material surrounding each

tissue site. The Boltzmann equation considers atomic and nuclear reaction processes in the propagation (transport) of a boundary source of particles through shielding in order to determine the particle flux, $\phi_j(x,E)$, of ion, j with energy, E and depth, x

$$\Omega \cdot \nabla \phi_j(x,\Omega,E) = \sum_k \int \sigma_{jk}(\Omega,\Omega',E,E')\phi_k(x,\Omega',E')dE'd\Omega' - \sigma_j(E)\phi_j(x,\Omega,E) \qquad (9)$$

The inclusive cross sections for absorption, σ_j, and fragmentation, knock-out elastic scattering etc., σ_{jk}, that enter in equation (9) are described elsewhere (Cucinotta *et al.,* 1998b). In equation (9), the boundary condition at $[x=0]$ is the space environment. We use the HZETRN code (Wilson *et al.*, 1991) solution of equation (9) in the risk uncertainty estimates we describe below.

In summing the total uncertainty from biological and physical factors, we assume the limiting value theory for combining many distributions as a normal distribution holds. The overall variance is then given by the sum of the squares of biological risk factors described above and the environmental and radiation transport uncertainties as

$$V_j(E) = F^2L^2\sigma^2_{biol} + R_0^2Q^2\sigma^2_{phys} + \sigma^2_{biol}\sigma^2_{phys} \qquad (10)$$

For the mixed-radiation fields in space we propagate the variance at depth, x in materials by summing over the energy spectra of each particle in the radiation field, $\phi_j(x,E)$

$$R_{total}(x) = \sum_j \int dE\,\phi_j(x,E)\;S_j(E)R_j(E) \qquad (11)$$

$$V_{total}(x) = \sum_j \int dE\,\phi_j(x,E)\;S_j(E)V_j(E) \qquad (12)$$

where, $S(E)$ is the stopping power. We assume that the median value of the distribution is not affected by uncertainties in the GCR environment or descriptions of radiation transport.

3.6 Environmental Uncertainty

The model of Badhwar and O'Neill (1992 and 1996) is used here to define the GCR radiation environment at a fixed time in the solar cycle. This model agrees well with satellite data from which it is derived and a root-mean-square error of < 10% is reported for protons and helium ions and a slightly higher error for heavy ions. We neglect any variation in uncertainties in individual components for environmental definition and assign an overall variance based on the expected uncertainty using a standard error of 15%,

$$\sigma_{envir} = [0.15]\ R(x) \tag{13}$$

where *R(x)* is the risk at depth, *x*. An additional uncertainty exists for treating the temporal variation of the GCR environment which will increase as the time between predictions and mission launch increases and is not considered here.

3.7 Transport Code Uncertainty

The assignment of an uncertainty in the description of radiation transport through shielding is complex since the uncertainty will be depth and material dependent, and with certain radiation components more uncertain than others. Materials with high atomic mass constituents increase in the role of secondary particle production and have been studied extensively in the past for proton and neutron transport. Materials such as hydrogen and carbon reduce the role of secondary particle production and projectile fragmentation is the dominant physical process for most shielding depths of interest. Here, fragmentation cross sections have been well studied in support of space science applications. Past measurements of the GCR on STS missions have agreed with transport measurements for integrated quantities such as dose and dose equivalent to within 25% for aluminum and polyethylene shielding (Badhwar and Cucinotta, 2000). Predictions of individual components have disagreed with measurements by factors from 2-5, however much of these differences are related to including detector response functions and it would be unrealistic to expect that the overall uncertainty in transport models is this large. We assume herein for charged particles an uncertainty that increases from a standard deviation of 10% at the entrance depth with a depth-dependent rate of 1% per g/cm^2 of material traversed by the radiation field,

$$\sigma^{Z}{}_{transport} = [0.1 + x/100] \quad R_z(x) \tag{14}$$

For neutrons we assume a higher range of uncertainty and use

$$\sigma^{n}{}_{transport} = [0.25 + x/50] \quad R_n(x) \tag{15}$$

Other uncertainties in physical definition include knowledge of the Mars atmosphere and lunar or Mars soil properties, and in the definition of spacecraft, surface habitat, and body-self shielding factors and are ignored in the present calculations.

3.8 RISK UNCERTAINTY PROJECTIONS

The upper level of acceptable risk for exploration has not been decided at this time. In the comparisons that follow we assume that a 3% excess fatal cancer limit, and note that this risk level is higher than the corresponding limit for LEO because it can be expected that selected astronauts for a Mars mission will have a significant prior radiation exposures from prior missions and training.

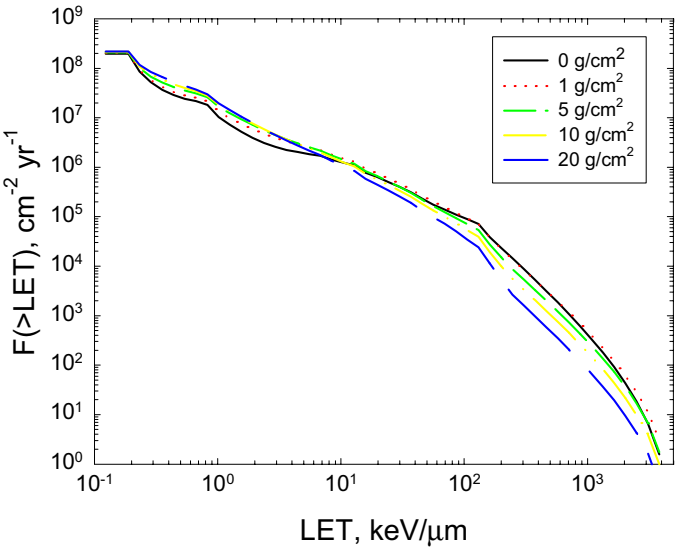

Figure 11: Integral LET spectra of GCR behind various amounts of shielding [data from Wilson *et al.,* 1995]

Also, the dose values corresponding to a 3% risk will be about 15% lower than that of Table 2 because the exposures will occur in a much shorter time-frame, while Table 2 assumes a dose distributed evenly over a 10-year career. The calculations use the GCR environmental model of Badhwar and O'Neill (1996), the HZETRN code (Wilson *et al.,* 1991; Wilson *et al.*, 1995) and the QMSFRG nuclear interaction model (Cucinotta *et al.,* 1996). For all calculations discussed, body-self shielding using the CAMERA model is assumed (Billings *et al.,* 1973; Yucker *et al.,* 1990). The change of the LET spectra with shielding plays a decisive role in our analysis and is illustrated in **Figure-11**.

Figure-12 shows results for the median risk and 95% confidence intervals (C.I.) versus depth in polyethylene and aluminum for 40–year-old males. The areal-density (units of g/cm^2) is the thickness divided by the density of the material and its use places each material on an equivalent mass scale. Although, polyethylene provides a reduction in comparison to aluminum shielding, the statistical significance of this reduction is masked by the large uncertainties. Therefore even though the differences in material effectiveness are realized using point-estimates as a basis for a determination, the large radiobiological uncertainties hinder positive arguments that can be made for many materials. Thus, narrowing the confidence intervals would enable designers to assess the improvements due to materials selection and optimize shielding mass for maximum protection and minimum costs. **Figure-13** shows the attenuation of risk for 40-year-old males and the 95% C.I. behind CO_2 shielding representing the Martian atmosphere for 1 year at solar minimum. We have used 4 g/cm^2 of aluminum shielding and the CAM model of BFO shielding in this comparison. The upper bound of the 95% C.I.s are well above the accepted level of career risks for LEO.

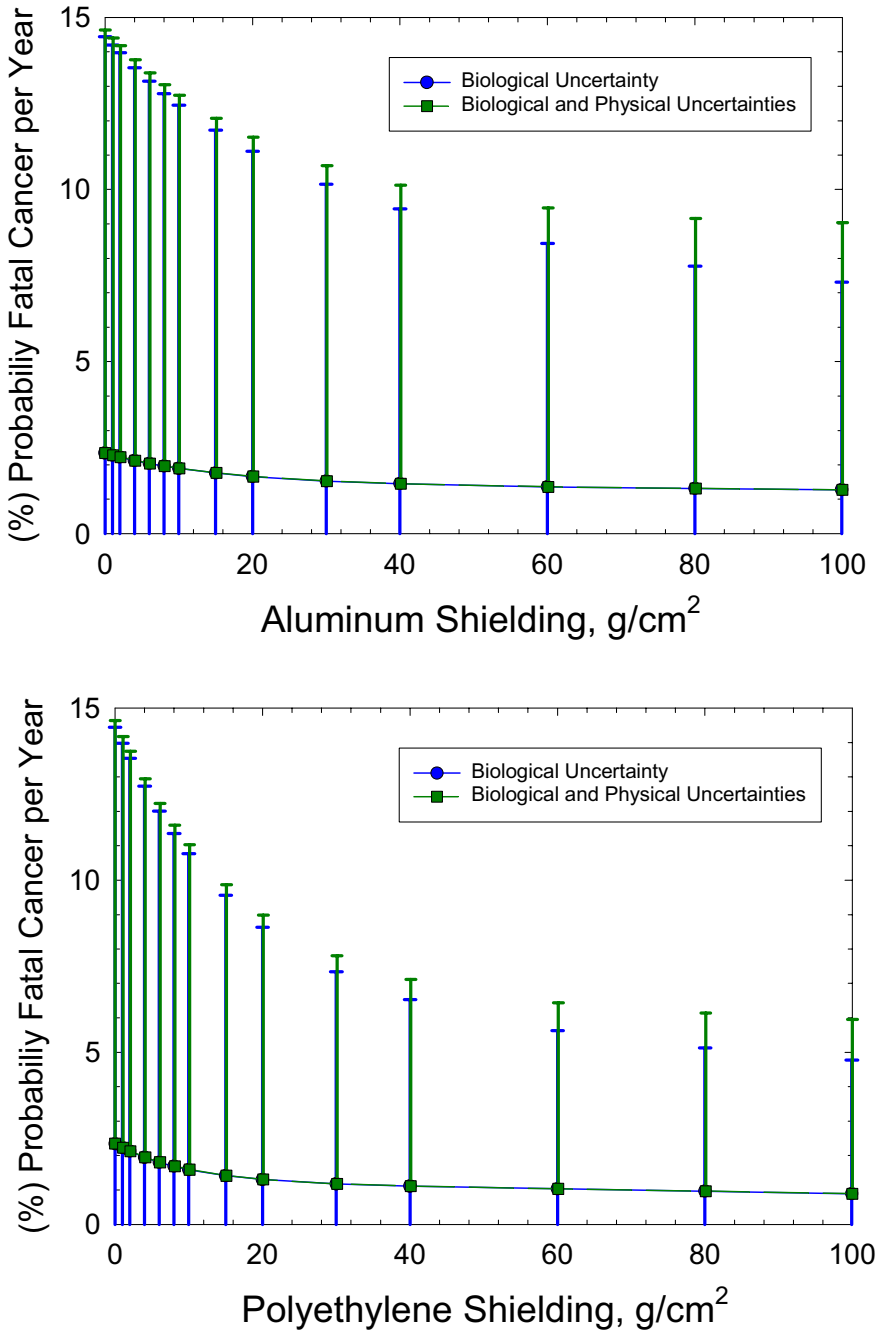

Figure 12: Median risk and 95% C.I. of fatal cancer for 40-year-old males for 1 year in space versus aluminum and polyethylene shielding depth.

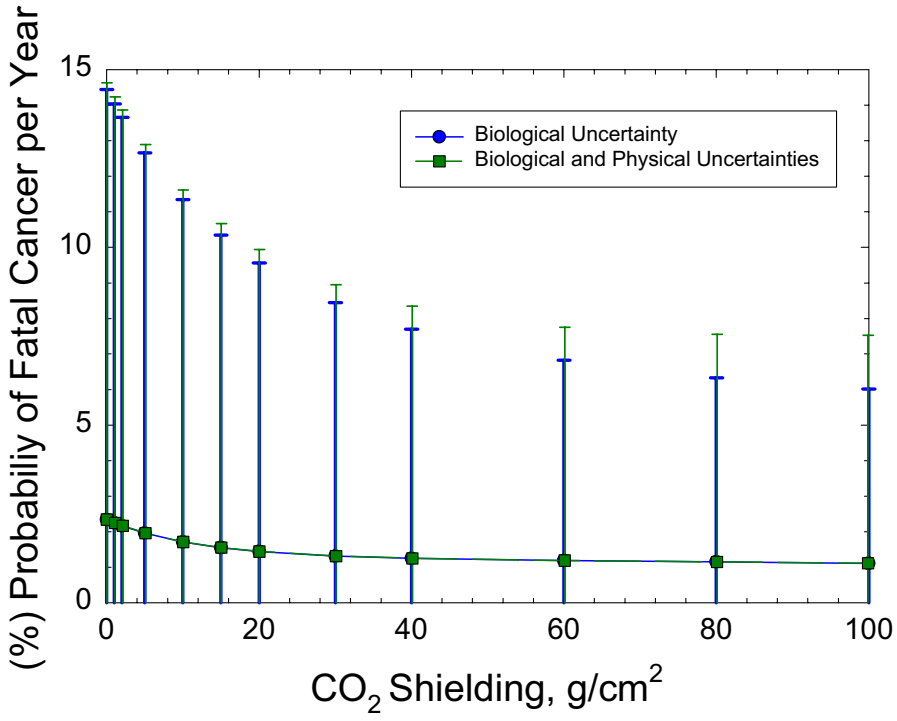

Figure 13: Median fatal cancer risk and 95% C.I. for 40-year-old males for a 1 year space mission as a function of varying amounts of CO_2 shielding.

The two classes of Mars missions most often discussed are called conjunction class and opposition class depending on whether the mid-point of the mission is closer to Mars conjunction (Mars in the Earth sky is closest to the sun) or Mars opposition (Mars is opposite of the Earth from the sun) (Chang Diaz, 2000; NASA-SP, 1997). The trajectories for these missions are illustrated in Figure-14. Conjunction class missions involve longer stay times at Mars (300-600 days) and one-way transit times of 150-250 days. Opposition class missions involve shorter Mars stays of 20-60 days, with one-way transit times of 100-400 days. The opposition class missions require higher energy requirements. Tables 10 and 11 show the calculations for 40-year-old females and males for several exploration scenarios. The comparison with the addition of 10 cm water shielding shows that the addition and optimization of shielding could lower risks to a level within the acceptable level of risk for

LEO astronauts, however the large uncertainties limit any conclusion on the acceptability of risk for long duration missions (> 100 d).

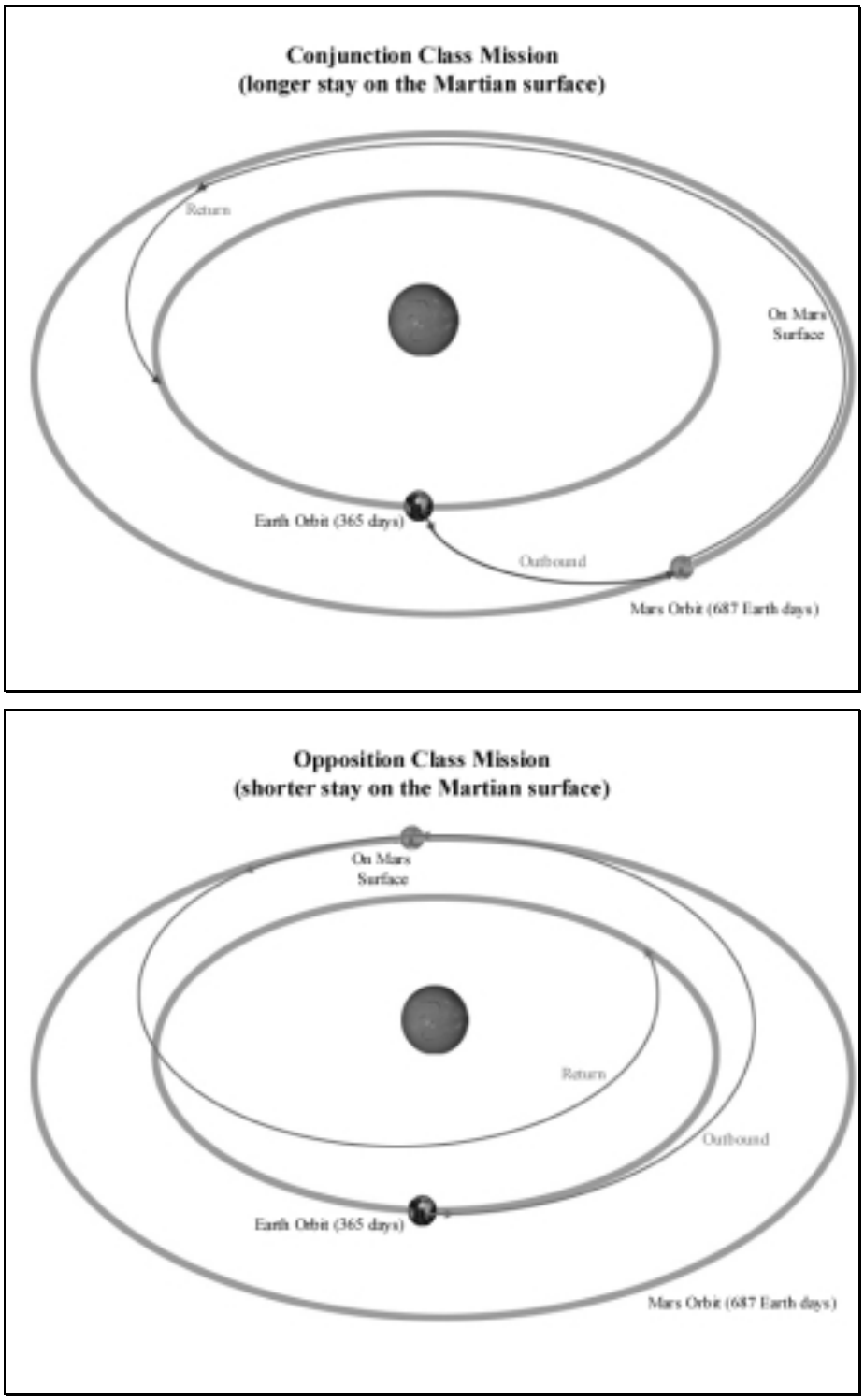

Figure 14: Conjunction and opposition classes of Mars mission possible scenarios.

Using age and gender dependent risk coefficients, we can estimate the number of days in space with a 95% C.I. to stay below a career risk of 3% excess cancer fatality can be assured. These estimates are shown in Table 12 and are made for solar minimum conditions. We have included the body self-shielding and 10 g/cm^2 of aluminum (typical spacecraft average) in this comparison. In **Figure-15** we show the level of confidence that is achieved for increasing times in space using aluminum, polyethylene, or hydrogen shielding (10 g/cm^2) for 45-year-old males. Also, shown in **Figure-15** are comparisons that include 400 days on the Mars surface using a high-density Mars atmosphere model (Simonsen *et al.,* 2000). It is not possible for crews of younger ages, especially females, to perform long duration missions with a significant safety factor based on the current estimate of uncertainties in risk projections.

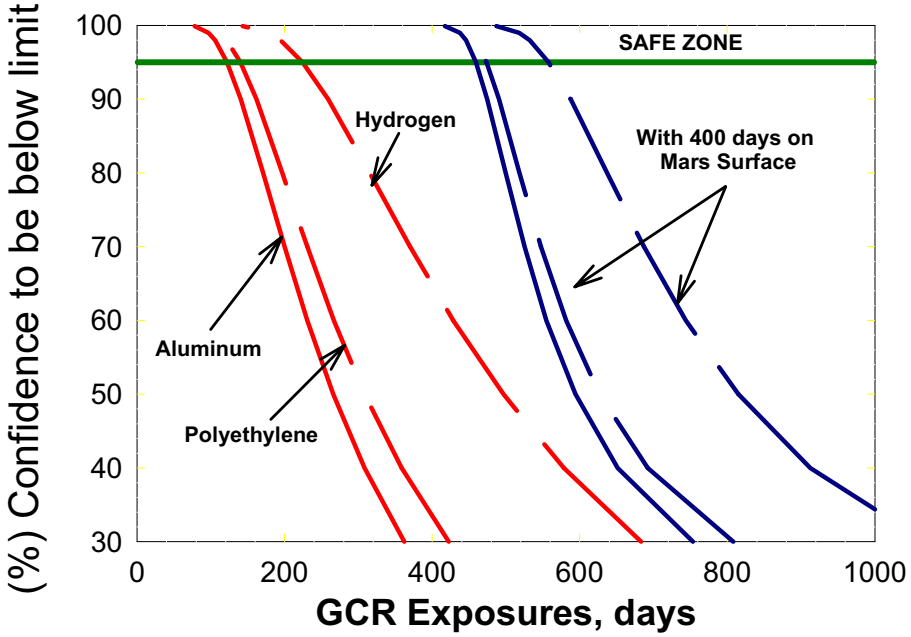

Figure 15: Confidence levels to stay below a 3% excess fatal cancer risk versus the number of days in free space or with 400 days on Mars surface for 45-year-old males.

The contributions of charge groups to the total risk and risk uncertainty provides important indicators for developing approaches to reduce cancer projection uncertainties. **Figure-16** shows the median and 95% C.I. for individual charge groups for a 40-year-old male using 4 g/cm^2 of aluminum shielding at depth in tissue. The medium and heavy charge groups dominate the overall uncertainties. The neutron contributions (z=0) shown include only the heavy ion recoils since the HZETRN code explicitly transports the recoil of hydrogen (z=1) and helium ions (z=2) produced by neutrons. Since neutrons make important contributions to the hydrogen and helium groups, it can be seen that reducing the uncertainties in neutron effects will make an important contribution to the overall uncertainty reduction.

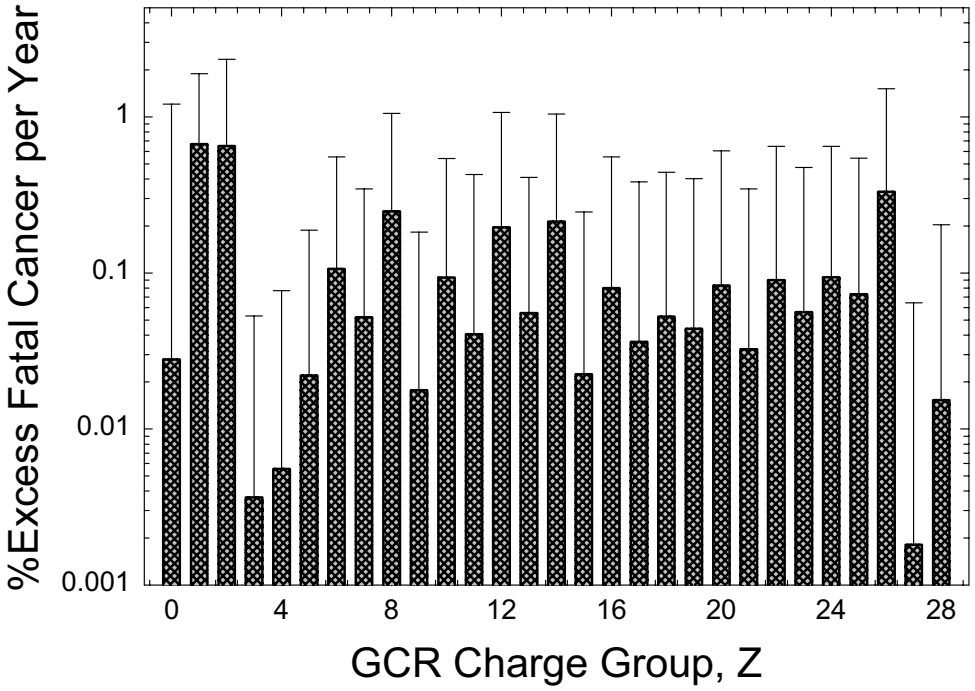

Figure 16: Confidence intervals for fatal cancer projection uncertainties for various GCR charge groups. These calculations are for 40-year-old males behind a 4 g/cm^2 aluminum shield.

Mission Type	Total Duration in Days (on Mars or lunar surface)	0 cm H_2O	10 cm H_2O
		% Probability of Excess Fatal Cancer	
Deep Space	62 (0)	0.6 [0, 3.3]	0.45 [0, 2.7]
Lunar Base	20 (14)	0.13 [0, 0.7]	0.09 [0, 0.6]
Mars-1	360 (30)	3.3 [0, 18.0]	2.5 [0, 14.6]
Mars-2	660 (30)	6.2 [0, 34.0]	4.6 [0., 27.5]
Mars-3	1000 (600)	5.7 [0, 30.8]	4.5 [0, 25.6]

Table 10: Fatal cancer risk projections and 95% C.I.s for 40-year-old females. Calculations are for several exploration type missions using 4 g/cm^2 aluminum shielding and high density Mars CO_2 atmosphere and considering effects of the addition of 10 cm water shielding. Values in parenthesis indicate days on Mars or lunar surface.

Mission Type	Total Duration in Days (on Mars or lunar surface)	0 cm H_2O	10 cm H_2O
		% Probability of Excess Fatal Cancer	
Deep Space	62 (0)	0.4 [0, 2.0]	0.27 [0, 1.6]
Lunar Base	20 (14)	0.08 [0,0.41]	0.06 [0, 0.34]
Mars-1	360 (30)	2.0 [0, 10.8]	1.5 [0, 8.8]
Mars-2	660 (30)	3.7 [0, 20.4]	2.8 [0, 16.5]
Mars-3	1000 (600)	3.4 [0, 18.5]	2.7 [0, 15.3]

Table 11: Fatal cancer risk projections and 95% C.I.s for 40-year-old males. Calculations are for several exploration type missions using 4 g/cm^2 aluminum shielding and high density Mars CO_2 atmosphere and considering effects of the addition of 10 cm water shielding. Values in parenthesis indicate days on Mars or lunar surface.

Age	Female (Projected Days)	Male (Projected Days)
30	54	91
35	62	104
40	73	122
45	89	148
50	115	191
55	159	268

Table 12: Projections of age and sex dependent maximum mission days in deep space for a 95% C.I. to stay below a 3% excess fatal cancer probability. Body self-shielding and 10 g/cm^2 aluminum shielding are assumed. Calculations are made near solar minimum where highest GCR exposures occur.

3.9 UNCERTAINTY REDUCTION

There are important prospects for reducing the uncertainties in risk projection in the future. New human cancer data from exposed cohorts will be one key element in risk uncertainty reduction. The study of cancer risks in the nuclear industry is an ongoing study involving several countries and will include a large population of workers (> 100,000) (Cardis *et al.*, 1995). In time, this database may replace that of the AB survivors because of its higher statistical power, and because the doses and dose-rates realized are better representative of occupationally exposed populations. This data will also allow tests of the predictive accuracy of the AB data. One aspect that would be of great benefit from new human data is to consider any tissue dependence on the DDREF for low-LET radiation. Past observations have noted a much larger DDREF for lung cancers than for e.g. breast cancer (NCRP, 2000). A confirmation of these results and an extension to other cancer types would be useful in reducing the uncertainties in the DDREF. There will also be new data available for second cancers from survivors of cancer treatments with proton and carbon beams, however this data will be less useful because it is not from a whole-body exposure and there exists a strong possibility of an inherent sensitivity of the patients.

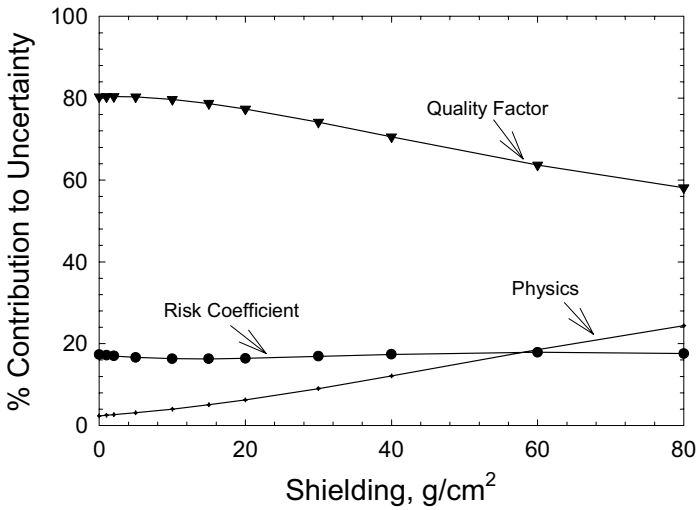

Figure 17: Contribution to the cancer projection uncertainty with increasing amounts of aluminum shielding.

The uncertainty in the dose-rate effects may be small for high-LET particles because there is very little dose-rate dependence observed experimentally or expected from biophysical considerations. However, in some cases an enhanced dose-rate effect is observed (Ullrich *et al.,* 1984; Ainsworth, 1982). An approach which considers PDFs for the DDREF that is dependent on radiation quality could be more accurate than the approach used here, but at odds with conventional risk assessment approaches. Experimental studies that focus on the DDREF for protons and heavy ions should provide a significant reduction in the current uncertainty levels. Tests of mixed radiation fields would also be useful. Aspects of mixed radiation fields are present in all experiments with high-energy beams due to nuclear reactions occurring in beam-lines or samples, and ŭ-ray events from cells that do not receive direct particle traversals. Studies with shielding materials can enhance the observation of possible mixed-field effects. However, the role of dose protraction is believed to be a more important uncertainty. Through the development of alternative forms of risk assessment, it may be possible to avoid this large contribution from dose-rate effects to the uncertainty in risk estimates. The use of a relative risk model that compares to acute gamma-ray data in animals and humans is a possible alternative approach that would avoid the large uncertainty in the DDREF for low-LET radiation. The physical doses to be incurred on exploration missions are accessible by experimental models (5-40 rad) and the dose-rate effects of protons may be the major uncertainty. The effects of nuclear reactions and track structure in tissue may not be properly estimated by existing data using *in vitro* models for estimating RBE.

Developing mechanistic models of heavy ion effects in conjunction with data collection in experimental models is the major approach to reduce risk uncertainties. Establishing a theoretical model that answers questions related to the linearity of effects at low dose-rates, the variation of sensitivity across tissue type, and the causal relationships between genomic instability and cancer will be needed. Also, a major challenge is how to apply knowledge from the recent revolutions in molecular biology and genetics (Vogelstein and Kinzler, 1997) for quantitative assessment of risks. The scarcity of data for late effects in animal models is a major barrier in providing estimates and hinder pre-Phase A or other design studies. The collection of data will also allow fundamental understanding cancer progression. An outline

of data collection timelines is described in a recent NAS Report (1997). The physical uncertainties estimated in the calculations above are much smaller than the biological ones. Until the uncertainties in biological factors are reduced significantly, it will be difficult to evaluate the importance of reductions in physical descriptions of radiation fields. Design studies for a manned mission to Mars are severely hampered until the biological uncertainties are reduced. Critical questions developed by scientists involved in NASA's Space Radiation Health Research Program are listed in Appendix B. It is believed that knowledge developed from research on answering these questions along with critical data collection are needed prior to the design of exploration class missions.

4. RISK MITIGATION

There are a number of approaches to reduce the potential radiation induced health risks in space flight including operational, shielding, and possibly biological countermeasures. In planning a strategy for risk reduction, the cost effectiveness of each area will need to be evaluated. Table 13 summarizes the expectation for each area to contribute to increases in the number of safe days in space where high confidence levels are assured and will allow NASA to reach its goal of the safe exploration of space. Improving risk assessment will potentially lead to a large gain in the number of days where an estimate of an acceptable level of risk with significant C.I.s could be achieved. Although the possibility exists for an increase in the expected risk from improved knowledge, we note that a narrowing of the uncertainty range even with increases in the median values would allow missions with acceptable risks to be designed. Funding of research to reduce the uncertainties in risk projections is expected to be the most cost-effective approach for reaching the goal of the safe exploration of space.

Approaches to increase the number of safe days projected for space exploration include restricting launch times within the course of the solar cycle and the development of advanced propulsion systems that significantly reduce the length of missions (Chang-Diaz, 2000). As shown above the role of improved radiation shielding is tied to the improvement of risk

assessment. The use of biological countermeasures to protect crewmembers would be a revolutionary strategy, however faces several obstacles. Based on ground-based experiences there is often a long time (10-25 years) between the initial science discoveries, clinical trials, and the use of a countermeasure. An exception would be biological countermeasures which have already been identified and could be tested with heavy ion beams in animal models in the near future. The efficiency of biological countermeasures would have to be quite high in comparison to those used on the ground in order to provide a significant benefit for a small number of individuals participating in exploration class missions. In contrast, for terrestrial exposures a moderate reduction can have an important benefit for reducing the risks of an important fraction of a larger population. Finally, as seen from Table 5, many tissues will contribute to the overall cancer risk from radiation exposure. Hence, a countermeasure that acts on a single or small number of tissues may only provide a small overall reduction in risk. On the other-hand, the development and use of methods that factor in an individuals genetic sensitivity or resistance to radiation would potentially play a large role in risk reduction.

Approach	Expected No. of Days Gained	Comment
Improved Risk Assessment	0-1000 days	Cost effective approach using data collection and research
Shielding and configuration optimization	50-300 days	Light mass materials identified, risk assessment data needed to improve approach, optimization needed early in design
Advanced Propulsion System	100-400 days	Large advantage if achievable
Crew Selection	50-300 days	Age, sex, genetic selection not ethical. Role of sensitivity to GCR not established at this time; CNS risks may increase with age
Biological Countermeasures	0-1000 days	Needs revolutionary research to achieve
Solar cycle variation	100-200 days	Reduces launch windows and increase SPE threats

Table 13: Estimates of increased number of safe days in space from improved risk assessment or risk mitigation approaches.

Because of the strong age and gender dependence of cancer induction, crew selection could reduce the probability of cancer, however such an approach may be counter to other mission goals. Also, the decreasing cancer risks with age of exposure may not be true for other health risks. The risks of damage to the central nervous system from space radiation are highly uncertain at this time (NAS, 1973; Joseph *et al.,* 1992; NAS, 1997; Tolifon and Fike, 2000). There is a strong possibility that if such risks are important that astronauts of older ages will be more susceptible to such effect because of the patterns of neuron loss with increasing age. Similarly, there is a small probability that a progressive cataract could arise during a long mission possibly impairing the crews ability to perform the mission. Although this possibility is small it could be larger for astronauts of older years.

4.1 Operational approaches

Operational approaches include using the knowledge of the radiation environment to reduce exposures including the selection of the launch-time within the solar cycle and the landing site on the Mars surface, and assuring adequate warning and protection from solar particle events (SPE). **Figure-18** shows the variation of the dose over the solar cycle (Wilson *et al.,* 1999a). Dose variations of more than a factor of two occur over the approximately 11-year solar cycle. Exposures could be reduced by optimization of the launch-time or by limiting mission duration. However, it is more likely that such windows will be out of phase with planetary alignments needed for a Mars launch. Also, a trade-off with increased probability of SPE occurs. Finally, it is likely that there will be multiple Mars missions with a good portion of the 10-12 year solar cycle being sampled by each mission.

Maximizing times on the Mars surface (conjunction class missions) could lead to significant risk reduction because of the shadow shielding provided by the Mars surface and because of the significant atmosphere on Mars. Surface maximization also favors science return and decreases the risk of the harmful effects of microgravity such as bone loss. The selection of a low altitude landing site would also favor risk reduction. **Figure-19** shows the Mars topographical map from the MOLA (Mars Orbiter Laser Altimeter) of the current MGS (Mars Global Surveyor) mission. Based on this most recent altitude data, radiation doses

were calculated that account for altitude variations over the Mars surface and are shown in the lower panel of **Figure-19**. **Figure-20** shows the change in skin dose equivalent for the individual hemispheres of Mars using the MOLA data (Smith *et al,* 1999). Optimization of landing sites with respect to the natural terrain of Mars can provide a significant reduction of risks on the Martian surface.

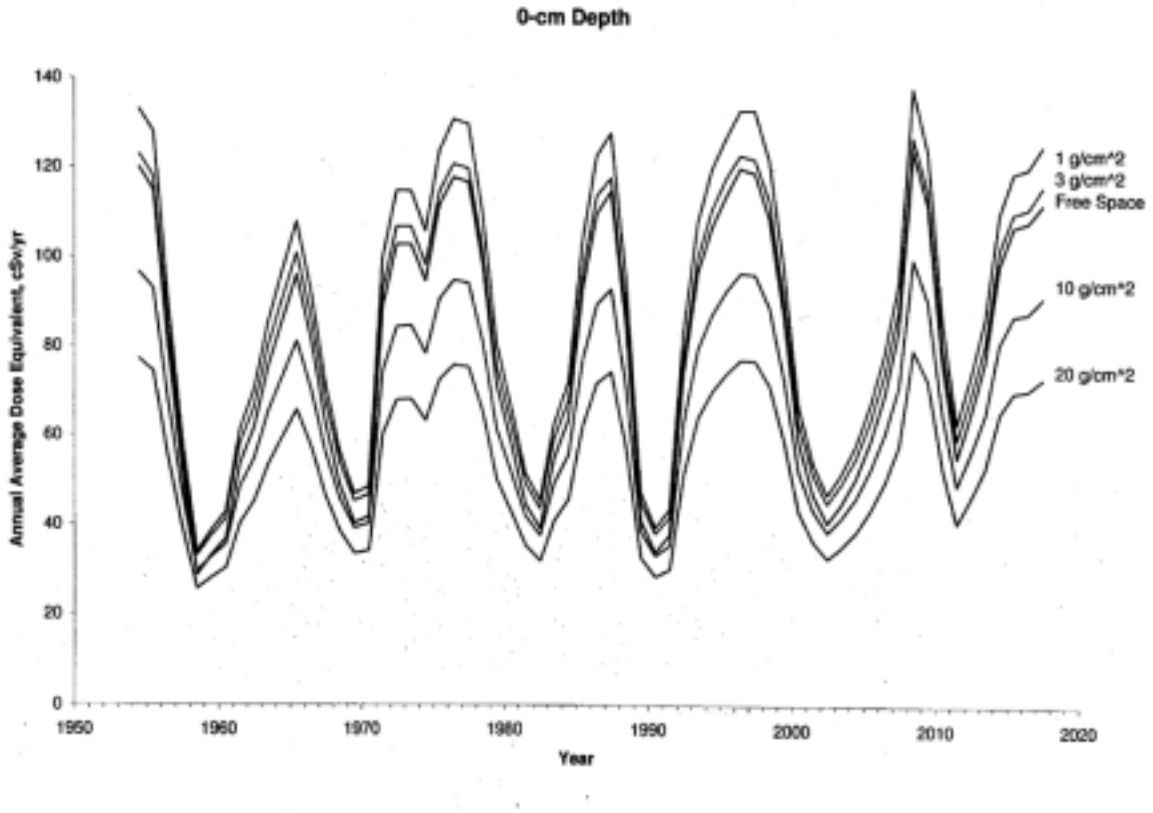

Figure 18: Variation of dose over a range of solar cycles behind various aluminum shields [Wilson *et al.,* 1996].

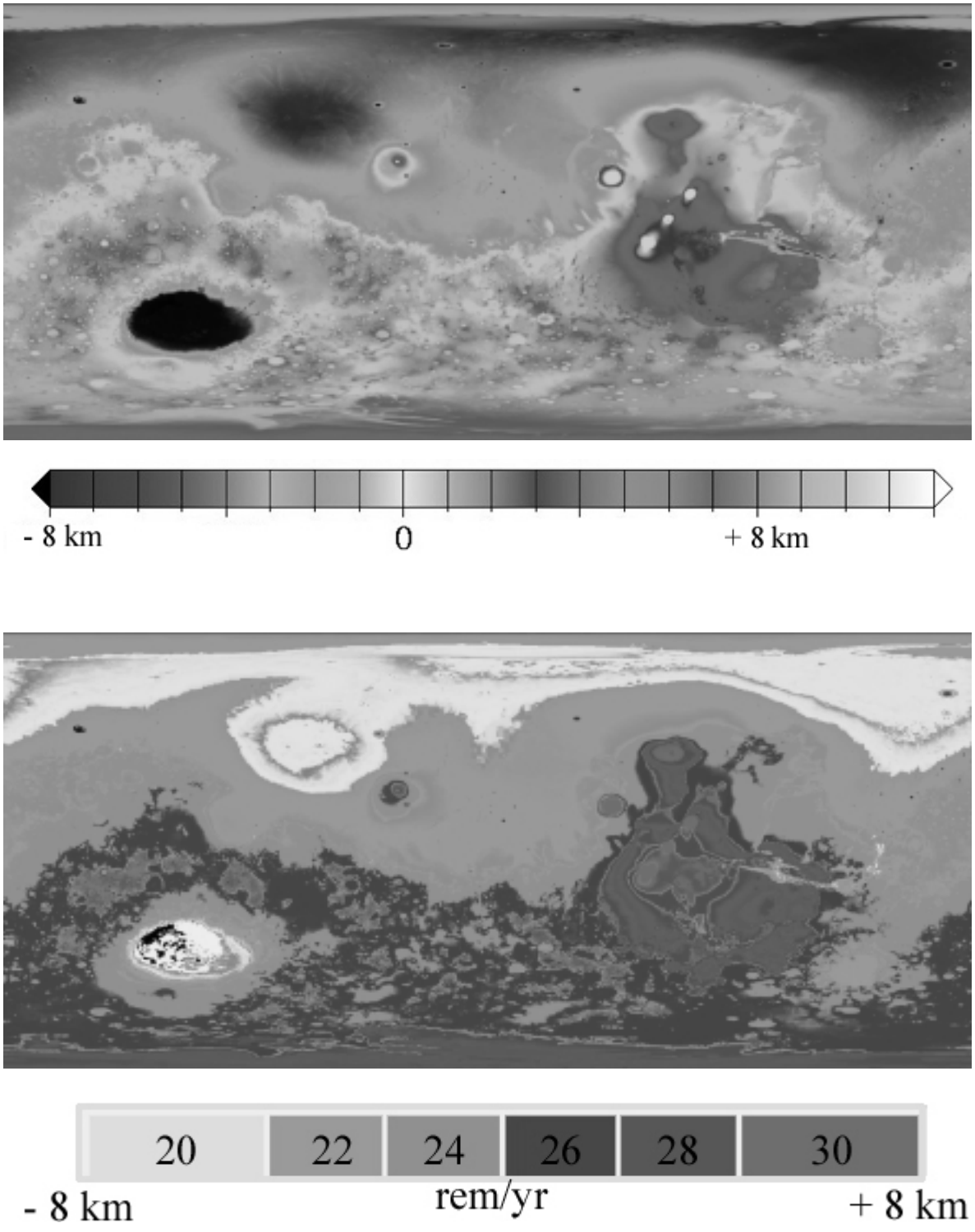

Figure 19: Topographical map of the Mars surface from the MOLA (Mars Orbiter Laser Altimeter) data from the MGS (Mars Global Surveyor) mission [data from Smith *et al.,* 1999]. Calculated radiation doses as a function of the altitude on the Mars surface with a high density CO_2 atmospheric model.

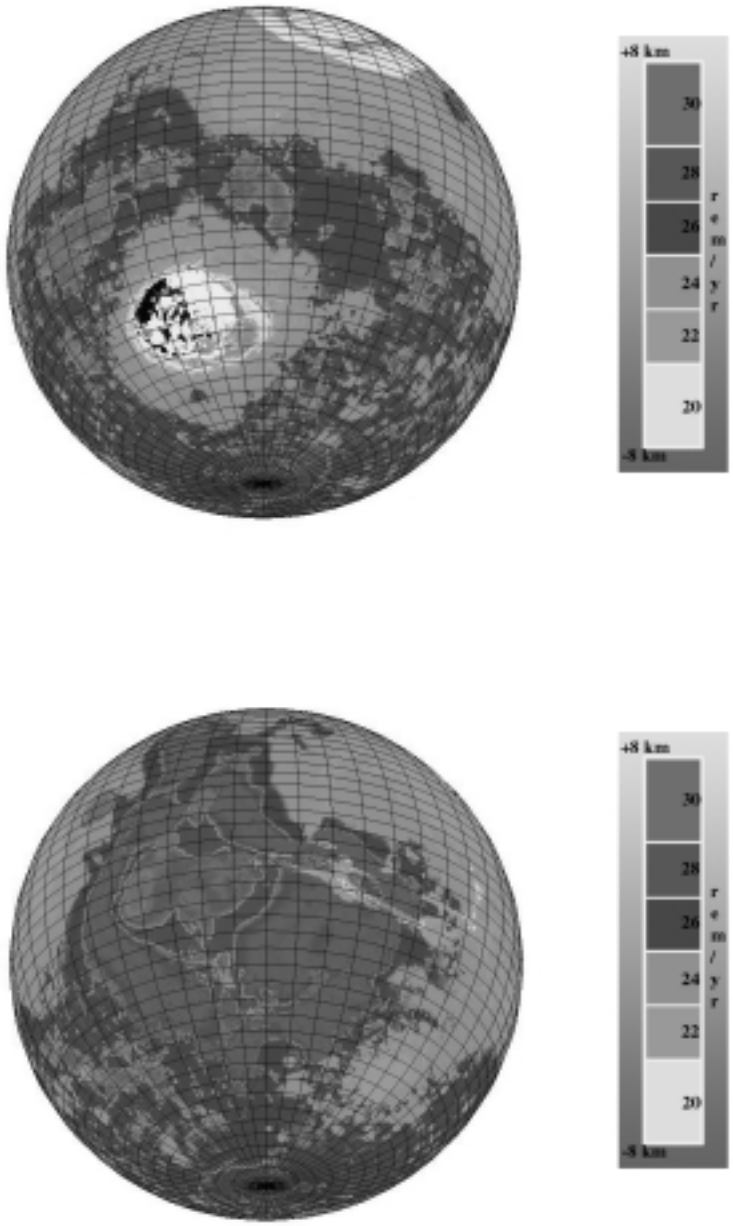

Figure 20: Variation of skin dose equivalent over the entire surface of Mars.

The largest solar particle events are associated with coronal mass ejections (CME). It is well known that the probability of solar particle events (SPE) is largest near solar maximum. Providing an effective early warning capability, alarm system, and protective storm-shelter would nearly eliminate any threats from solar particle events. The radial gradient associated with CMEs and shock acceleration is not well understood. The radial gradient is most pronounced in the inner-heliosphere and is believed to be due to the initial near-sun particle injection and radiation propagation from the Sun along the interplanetary field lines (Smart and Shea, 1992). In the outer-heliosphere, the gradient should be dominated by the major interplanetary field structures. Sensors should be able to detect shock acceleration from a CME for perhaps up to about 8 hours prior to the shock waves arrive at the spacecraft or Mars surface. The ESA/NASA SOHO spacecraft can image a CME to a distance of 30 solar radii. Networks of satellites that can provide imaging capabilities for spacecraft en route to Mars and on the Mars surface have been proposed (Feynman, 1999).

The use of low atomic mass materials for a SPE storm shelter could reduce the overall shielding mass requirements of a mission. Wilson *et al.* (1999a) have shown that the dose equivalent from the historically largest SPEs can be effectively reduced using polyethylene shielding (reproduced in Table 14). This comparison shows that the use of light atomic mass materials can significantly reduce the acute risk from an SPE. An important factor for SPE planning will be the time allowed for EVA crews on the lunar or Mars surface. The greatest threat will come on the lunar surface since a significant atmosphere protects the Mars surface. Even with an adequate alert system, only 1-2 hours of time may be available to seek shelter on the lunar surface before a high dose is received. For EVAs on Mars, 2-3 hours could be allowed however, shorter response times would be preferred.

4.2 Shielding Mitigation

The second approach for risk mitigation is to provide effective radiation shielding. Shielding is potentially a very useful approach to mitigation since limiting mission duration or selecting restricted years in the solar cycle are counter-productive for long range plans of space exploration. Theoretical and computational efforts in the late 1980s and early 1990s have

provided the basic understanding needed to design effective shielding approaches (Wilson *et al.*, 1995). The use of materials of low atomic mass and high hydrogen content are the key to shielding effectiveness because of the high energies of cosmic rays where nuclear secondaries are produced with large multiplicity. Low atomic mass materials reduce the occurrence of secondary particle production (neutrons, protons, and heavy ion recoils) and are also more effective per unit mass of material in slowing down and stopping heavy ions in atomic collisions. Validation of this approach has been made on the Space Shuttle by employing spheres of aluminum and polyethylene of similar areal-density. **Figure-21** shows measurements of the dose equivalent inside aluminum and polyethylene spheres on the STS-81 and STS-89 missions. The data was collected using an active tissue equivalent proportional counter (TEPC) that isolated the GCR contributions (Badhwar and Cucinotta, 2000). This experiment showed that aluminum provides no protective effects in reducing the dose equivalent of the GCR in LEO, while polyethylene was an effective absorber of GCR. NASA should develop shielding technologies to use high hydrogen content polymers for spacecraft and local shielding of sleep stations or other high-crew occupancy areas of spacecraft. Such technologies will play a vital role and cost effective approach in allowing for safe exploration of Mars and other planetary bodies in the future. A key factor will be to include shielding optimization as early as possible in vehicle design using an integrated design approach.

	Aluminum Structure		**Polyethylene Structure**	
Organ	Equipment Room (Sv)	Shelter (Sv)	Equipment Room (Sv)	Shelter (Sv)
Skin	4.27	1.1	2.67	0.58
Lens	3.67	1.01	2.51	0.57
BFO	0.65	0.24	0.5	0.16

Table 14: Organ dose equivalent in aluminum and polyethylene structures for the August 1972 SPE [Wilson *et al.,* 1999a].

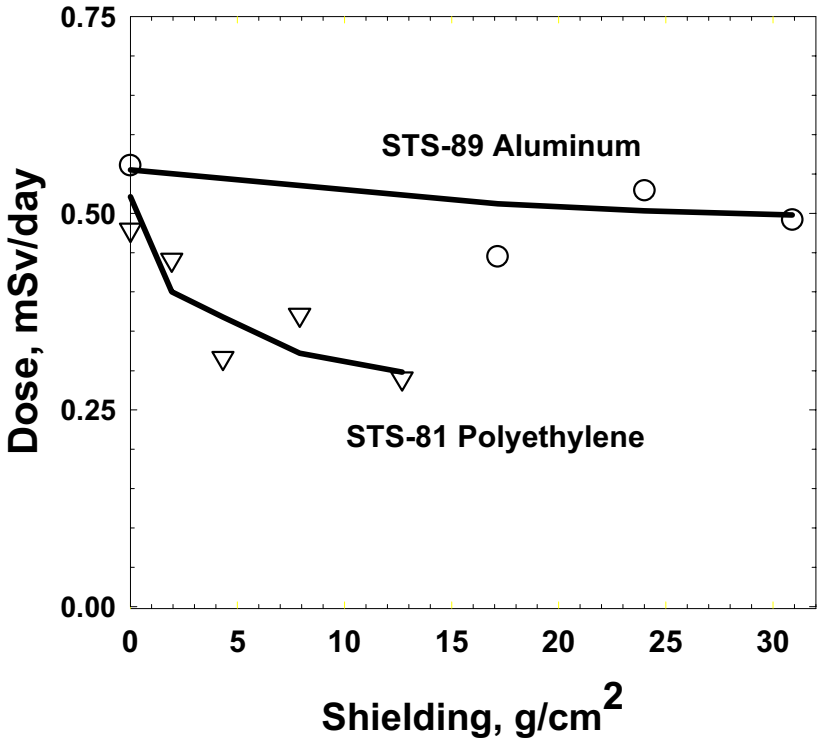

Figure 21: Comparisons of calculations to measurements using aluminum and polyethylene spheres flown on STS-81 and STS-89, respectively [Badhwar and Cucinotta, 2000].

4.3 Biological Countermeasures

The understanding of the molecular basis of radiation action is expected to lead to biological countermeasures for risk mitigation (LBNL, 1997). An effective countermeasure for space radiation must work for extended periods of time, be effective for high-LET radiation, and can lead to only minor side effects. In the discussion above on the biological action of heavy ions the possibility of unique mechanisms of biological damage in comparison to terrestrial radiation were noted. How such mechanisms impact the efficiency of radioprotectors will be an important issue. The validation of biological countermeasures will require extensive testing with protons and heavy ions. Ground-based research facilities capable of simulating the radiation that occurs in space are essential in order to make these advances. After many years of limited access to such facilities, NASA is developing a dedicated facility called the

Booster Application Facility (BAF) at the Department of Energy's (DOE), Brookhaven National Laboratory (BNL) in Upton, NY. The BAF will play a critical role in the development of safe and effective biological countermeasures. Table 15 lists the range of energies and particle types that will be accessible to NASA funded investigators using the BAF. Clearly the range of the BAF covers the particle types and energies of interest for GCR and SPE studies.

It is not known if radioprotectants developed for low-LET radiation would be effective for heavy ions and neutrons. Both acute and late effects are of concern during space flight, and may call for distinct approaches. Radioprotectors have been developed in the past by the military for protection during an atomic bomb blast and in radiation cancer therapy for the purpose of reducing the effects to normal tissues in patients. Acute effects are possible following a large solar particle event, and since low-LET protons would dominate exposures, it is expected that these approaches may be effective for preventing acute radiation syndromes. At the molecular level, many protectors function as radical scavengers or in preventing hydrogen transfer. A second approach considers promotion of the recovery of stem-cell populations in highly renewable tissues, which can help deter acute tissue responses. A large number of chemical compounds were developed and tested at the Walter Reed Army Institute of Research in the 1960s and 1970s. The compound WR-2721 was shown to be quite effective in reducing acute radiation effects, however the use of WR-2721 and other phosphorothioates leads to serious side effects including vomiting and vasodilatation (NCRP, 1989). It has been shown that the combination of WR-2721 and the compound WR-1065 reduces mutation following both gamma ray and neutron exposures (Grdina *et al.*, 1992) perhaps though promotion of apoptosis in damaged cells. Such studies are useful for SPE protection since they show that such compounds could be effective if taken immediately after a SPE exposure was incurred.

A promising approach in the use of radioprotectors is being pursued which combines lower doses of radioprotectors with dietary factors that include anti-oxidants such as vitamin E and A (Pence and Yang, 1999). The use of lower doses is expected to reduce the potential of side effects. Special attention needs to be made to deficiencies in vitamins that may occur because

of other space flight stress (Pence and Yang, 1999). Altered cytokine expression due to microgravity may also play a role.

Although, anti-oxidants may be ineffective in reducing initial DNA damage from high-LET radiation, the role of persistent ROS as an induced process following radiation exposure (Polyak *et al.*, 1997; Fornace *et al.*, 2000) suggests that anti-oxidants may provide some benefit for reducing late effects. The use of anti-proteases (Kennedy *et al.,* 1996) or gene therapy approaches which function to promote apoptosis or extend cell cycle arrests such as the inhibitor p21 or members of the BAX family or genes, have been suggested in the past for low-LET radiation and these approaches should be considered for high-LET radiation as well (LBNL, 1997). Anti-oxidants have been tested for reducing heavy ions effects (iron) by Burns *et al.,* (2001) for rat skin cancer and Rabin *et al.,* (2000) for the down regulation of altered dopamine expression in the rat CNS. These studies have found a significant reduction in the effects of iron particles. Such studies must be continued using other heavy ion types with improved statistics (more animals) and to study the dependence on concentration to validate the approach. Also, fundamental understanding will be needed prior to use in humans.

Ions	Charge State in the Booster	Kinetic Energy Range (GeV/u)	Estimated Maximum Intensity (10^9 ions per pulse)
Protons	1	0.1-3.07	100
Helium	2	0.1-2.2	50
Carbon	6	0.1-1.6	20
Silicon	14	0.1-1.23	4
Iron	21	0.1-1.1	0.4
Copper	22	0.1-1.04	1
Gold	32	0.04-0.3	2

Table 15: Examples of particle energies and type to be accelerated at the Booster Applications Facility (BAF).

Finally, the use of chemopreventers that function to inhibit the promotional effects of both radiation and pre-malignant clones in a target tissue should be considered. One such study is underway by the National Space Biomedical Research Institutes (NSBRI) Radiation Effects Team using the agent tamoxifen and the rat mammary model (Dicello *et al.*, 1999). Tamoxifen is a non-steroidal drug belonging to the triphenylethylene class of compounds,

which functions as an estrogen antagonist in rats and humans. Rats are being exposed to photons, protons, and iron particles in order to test the effectiveness of tamoxifen in reducing tumors for each radiation type. Early results have shown that a significant reduction in mammary tumor incidence is found in rats treated with tamoxifen and irradiated with iron ions. Another agent that shows promise for reducing the carcinogenic effect of radiation is the compound buthionine-SR-sulfoximine (BSO). BSO down regulates the ras-raf-MAPK signaling pathway. Point mutations in the *ras* and *raf* genes proto-oncogenes are a common early event in many human cancers. BSO has been show to be effective in reducing lung-tumors and leukemia as demonstrated in a mouse model (Miller *et al.*, 1999). As other agents are being developed to the stage of human clinical trials by the National Institute of Health (NIH) or others, studies at BAF with animal models may be appropriate.

4.4 Genetic Variability and Risk Mitigation

Genetic variability will play an important role in understanding risk estimates and in the development of biological counter-measures. Many gene mutations and DNA polymorphisms that play a role in DNA repair and replication, cell cycle control, and cell signaling have now been identified (Vogelstein and Kinzler, 1997). Although homozygotes for such genetic defects are rare in the population, heterozygotes may make-up a substantial fraction of the general population for one or more factors that play a role in both sensitive or resistant radiation pre-dispositions (Vogelstein and Kinzler, 1997; Fornace *et al.,* 1999). Large-scale gene microarrays using mRNA extracted from cells or tissues are now available to study the expression of many thousands of genes and their role in responses to radiation (Fornace *et al.,* 1999; DeRisi *et al.,* 1997; LBNL, 1997). Bio-informatics approaches are being developed to understand the information content of such data (Fornace *et al*., 1999, Eisen *et al.,* 1998). Potential uses of these approaches are in the study of epidemiological data of exposed cohorts and the variations in sensitivity for e.g. across mouse strains. Individual differences will also be important in the development of biological countermeasures and for understanding their potential effectiveness. Important ethics questions will need to be addressed in the future to determine how such knowledge can appropriately be applied for space exploration.

5. REFERENCES

Ainsworth, E.J., Radiation Carcinogenesis Perspectives, In: Probability Models and Cancer, ed. L. LeCam, J. Neyman, North-Holland Publishing Company, Amsterdam, 99-170, 1982.

Ainsworth, E.J., Early and Late Mammalian Responses to Heavy Charged Particles, *Adv. in Space Res.* **6**, 153-162, 1986.

Alpen, E.L., Powers-Risius, P, Curtis, S.B., and DeGuzman, R., Tumorigenic Potential of High-Z, High-LET Charged Particle Radiations. *Radiat. Res.* **88**, 132-143, 1993.

Anonymous, Strategic Program Plan for Space Radiation Health Research. NASA Office of Life Sciences and Microgravity Applications, Washington D.C., 1998.

Badhwar, G.D., and O'Neill, P.M., An Improved Model of GCR for Space Exploration Missions, *Nucl. Tracks Radiat.* Meas. **20**, 403-410, 1992.

Badhwar, G.D., and O'Neill, P.M., GCR Model and its Applications, *Adv. Space Sci.***17**(2), 7-17, 1996.

Badhwar, G.D., and Cucinotta, F.A., A Comparison on Depth Dependence of Dose and Linear Energy Transfer Spectra in Aluminum and Polyethylene, *Radiat. Res.* **153**, 1-8, 2000.

Barcellos-Hoff, M., How Do Tissues Respond to Damage at the Cellular Level? The Roles of Cytokines in Irradiated Tissues. *Radiat. Res.* **150**, S109-S120, 1998.

Belli, M., Cera F., Cherubini R., Haque, A.M.I., Ianzini, F., Moschini, G., Sapora, O., Simone, G., Tabocchini, M.A., Tiverton, P., Inactivation and Mutation Induction in V79 Cells by Low Energy Protons: Re-evaluation of the results at the LNL facility, *Int. J. Radiat. Biol*. **63**, 331-337, 1993.

Billings, M.P., Yucker, W.R., and Heckman, B.R., Body Self Shielding Data Analysis, McDonnell Douglas Astronautics Company West, MDC-G4131, 1973

Borek, C., E.J. Hall, and H.H. Rossi, Malignant Transformation In Cultured Hamster Embryo Cells Produced By X-Rays, 430 keV Mono-Energetic Neutrons, And Heavy Ions. *Cancer Res.* **38**, 2997-3005, 1978.

Broerse, J.J., Davellar, J., and Zurcher, C., Tumor Induction in Animals and the Radiation Risk for Man. In Biological Effects of Solar And Galactic Cosmic Radiation, Part A (C.E. Swenberg, G. Horneck, and E.G. Stassinopoulos, Eds.) 161-175, Plenum Press, NY, 1993.

Burns, F., Yin Y., Garte, S.J., and Hosselet, S., Estimation of Risk Based on Multiple Events in Radiation Carcinogenesis of Rat Skin. *Adv. Space Res.* **14**, 507-519,1994.

Burns, F., Zhao P., and Xu G., Cancer Induction in Rat Skin Following Single or Multiple Doses of 1.0 GeV/nucleon ^{56}Fe Ions from the Brookhaven Alternating Gradient Synchrotron, *Phys. Med*. (in press), 2001.

Cardis, E., *et al.*, Effects of Low Doses and Dose-rates of External Ionizing Radiation: Cancer Mortality Among Nuclear Industry Workers in Three Countries. *Radiat. Res.* **142**, 117-132, 1995.

Chang-Diaz, F.R., The VASIMR Rocket, Scientific American, **283** (5), 90-97, 2000.

Cucinotta, F.A., Katz, R., Wilson, J.W., Townsend, L.W., Shinn, J.L., and Hajnal, F., Biological Effectiveness of High-Energy Protons: Target Fragmentation. *Radiat. Res.* **127**, 130-137, 1991.

Cucinotta, F. A., and Wilson, J. W., Initiation-Promotion Model of Tumor Prevalence in Mice from Space Radiation Exposures. *Radiat. and Environ. Biophys.* **34**, 145-149, 1995.

Cucinotta, F.A., Wilson, J.W., Shavers, M.R., and Katz, R., Effects of Track Structure and Cell Inactivation on the Calculation of Heavy Ion Mutation Rates in Mammalian Cells. *Int. J. Radiat. Biol.* **69**, 593-600, 1996.

Cucinotta, F.A., Nikjoo, H., and Goodhead, D.T., The Effects of Delta Rays on The Number of Particle-Track Traversals per Cell in Laboratory and Space Exposures, *Radiat. Res.* **150**, 115-119, 1998a.

Cucinotta, F.A., Wilson, J.W., Shinn, J.L., and Tripathi, R.K., Assessment and Requirements of Nuclear Reaction Data Bases for GCR Transport in the Atmosphere and Structures. *Adv. Space. Res.* **21**, 1753-1762, 1998b.

Cucinotta, F.A., Nikjoo, H., and Goodhead, D.T., Applications of Amorphous Track Models in Radiobiology, *Radiat. Environ. Biophys.* **38**, 81-92, 1999a.

Cucinotta, F.A., Wilson, J.W., Williams, J.R., and Dicello, J.F., Analysis of Mir-18 Results for Physical And Biological Dosimetry: Radiation Shielding Effectiveness In LEO. *Radiat. Meas.* **31**, 2000a.

Cucinotta, F.A.; Nikjoo, H.; and Goodhead, D.T.: Radial Distribution of Energy Imparted in Nanometer Volumes from HZE Particles, *Radiat. Res.*, **153**, 459-468, 2000b.

Cucinotta, F.A., Nikjoo, H., O'Neill, P., and Goodhead, D.T., Kinetics of DSB Rejoining and the Formation of Simple Exchange Aberrations. *Int. J. Radiat. Biol.* **76**, 1463-1474, 2000c.

Cucinotta, F.A., and Dicello, J.F., On the Development of Biophysical Models for Space Radiation Risk Assessment. *Adv. Space. Res.* **25**, 2131-2140, 2000d.

DeRisi, J.L., Vishwanath, R., Iyer, R., Brown, P.O., Exploring the Metabolic and Genetic Control of Gene Expression on Genomic Scale, *Science,* **278**, 680-686, 1997.

Desphande, A., Goodwin, E.H., Bailey, E.H., Marone B.L., Lehnert, B.E., A-Particle-Induced Sister Chromatid Exchange in Normal Human Lung Fibroblasts: Evidence for an Extra Cellular Target. *Radiat. Res.* **145**, 260-267, 1996.

Dicello, J.F., Cucinotta, F.A., Gridley, D.S., Howard, S.P., Novak, G.R., Ricart-Arbona, R., Strandberg, J.D., Vazquez, M.E., Williams, J.R., Zhang, Y., Zhou, H., and Huso, D.L., Carcinogenesis in Sprague-Dawley Rats Irradiated with Iron Ions, Protons, or Photons, In Proceedings of the First Biennial Space Biomedical Investigators Workshop, 1999.

Edwards, A.A., RBE of Radiations in Space and the Implications for Space Travel. *Phys. Med.* (in press) 2001.

Eisen, M.B., Spellman, P.T., Brown, P.O., Botstein, D., Cluster Analysis and Display of Genome-Wide Expression Patterns. *Proc. Natl. Acad. Sci*. **95**, 14863-14868, 1998.

English, R.A., and Liles, E.D., Iridium and Tantalum Foils for Space-flight Neutron Dosimetry. *Health Phys.* **22**, 503-507, 1972.

Ernhart, E.J., Gillette, E.L., and Barcellos-Hoff M.H., Immunohistochemical Evidence for Rapid Extra Cellular Matrix Remodeling after Iron-Particle Irradiation of Mouse Mammary Gland. *Radiat. Res.,* **145**, 157-162, 1996.

Feynman, J., and Ruzmaikin, A., Problems in the Forecasting of Solar Particle Events for Manned Missions, *Radiat. Meas*. **30**, 275-280, 1999.

Fornace, A.J., Amundson, S.A., Bittner, M., Myers, T.G., Meltzer, P., Weinstein, J.N., Trent, J., The Complexity of Radiation Stress responses: Analysis by informatics and Functional Genomics Approach, *Gene. Expr.* **7** (4-6), 387-400, 1999.

Fornace, A.J., Fuks, Z., Weichselbaum, R.R., Milas, L., Radiation Therapy. In: The Molecular Basis of Cancer, Second Addition, ed., Mendelsohn, J., Howley, P.M., Israel, M.A., and Liotta, L.A., W. Saunders, Philadelphia, 2000.

Friedberg, E.C., Walker, G.C., and Siede, W., DNA Repair and Mutagenesis. ASM Press, Washington D.C., 1995.

Fry, R.J.M., Powers-Risius, P., Alpen, E.L., and Ainsworth, E.J., High-LET Radiation Carcinogenesis, *Radiat. Res.* **104**, S188-195, 1985.

Fry, R.J.M., and Storer, J., External Radiation Carcinogenesis, *Adv. in Radiat. Biol.* **13**, 31-90, ed. J.T. Lett (New York, Academic Press), 1987.

Goodhead, D.T., Initial Events in the Cellular Effects of Ionizing Radiations: Clustered Damage in DNA. *Int. J. Radiat. Biol.* **65**, 7-17, 1994.

Grdina, D.J., Kataoka, Y., Basic, I., and Perrin, J., The Radioprotector WR-2721 Reduces Neutron-Induced Mutations at the Hypoxanthine-guanine Phosphoribosyl Transferase Locus in Mouse Splenocytes when Administered Prior to of Following Radiation. *Carcinogenesis* **13**, 811-814, 1992.

International Commission on Radiation Protection Publication 60, 1990 Recommendations of the International Commission on Radiological Protection. Pergamon Press, Oxford, 1991.

International Commission on Radiation Units, The Quality Factor in Radiation Protection, ICRU Report 40, ICPU Publications, Bethesda, MD, 1986.

Joseph, J.A., Hunt, W.A., Rabin, B.M., and Dalton, T.K., Possible "Accelerated Striatal Aging" Induced by ^{56}Fe Heavy Particle Irradiation: Implications for Manned Space Flights. *Radiat. Res.* **130**, 88-95, 1992.

Katz, R., Ackerson B., Homayoonfar M., and Scharma S.C., Inactivation of Cells by Heavy Ion Bombardment. *Radiat. Res.* **47***,* 402-425, 1971

Kanaar, R., and Hoeijmakers, J.H.J., Recombination and Joining: Different Means to the Same Ends. *Genes and Function* 1, 165-174, 1997.

Kawata, T., Durante, M., Furusawa, Y., George, K., Takai, N., Wu, H., Cucinotta, F.A., Initial G2-Chromosome Damage Induced in Normal Human Fibroblasts by High-LET Particles*. Int. J. Radiat. Biol.* (In press), 2001.

Kennedy, A.R., Beazer-Barclay, Y., Kinzler, K.W., Newberne, P.M., Suppression of Carcinogenesis in the Intestines of Min Mice by the Soybean-Derived Bowman-Birk Inhibitor. *Cancer Res.* **15**, 679-682, 1996.

Kiefer, J., Stoll, U., and Schneider, E., Mutation Induction by Heavy Ions. *Adv. Space Res*. 14, 257-265, 1994.

Khadim, M.A., MacDonald, D.A., Goodhead, D.T., Lorimore, S.A., Marsden, S.A., and Wright, E, Transmission of Chromosomal Instability After Plutonium Alpha Particle Irradiation. *Nature* **355**, 738-740, 1992.

Kranert, T., Schneider, E., Kiefer,. J., Mutation Induction in V79 Chinese Hamster Cells by Very Heavy Ions, *Int. J. Radiat. Biol.* **58**, 979-987, 1990.

Kronenberg, A., and Little, J.B., Locus Specificity for Mutation Induction in Human Cells Exposed to Accelerated Heavy Ions. *Int. J. Radiat. Biol.* **55**, 913-924, 1989.

Lawrence Berkeley National Laboratory Report LBNL-40278, Modeling Human Risk: Cell and Molecular Biology in Context, 1997.

Lett, J.T., and Williams, G.R., Effects of LET On The Formation and Fate of Radiation Damage to Photoreceptor Cell Component of the Rabbit Retina: Implications for the Projected Manned Mission to Mars. In Biological Effects of Solar and Galactic Cosmic Radiation, Part-A (C.E. Swenberg, G. Horneck, and E.G. Stassinopoulos, Eds.) 185-201, Plenum Press, NY, 1993.

Lobrich, M., Rydberg, B., and Cooper, P.K., Repair of X-Ray Induced DNA Double Strand Breaks in Specific *Noti* Restriction Fragments in Human Fibroblasts: Joining of Correct and Incorrect Ends. *Proc. Nat. Acad. Sci. USA*, **92**, 12050-12054, 1995.

Martin, S.G., Miller, R.C., Geard, C.R., Hall, E.J., The Biological Effectiveness of Radon-Progeny Alpha Particles. IV. Morphological Transformation of Syrian Hamster Embryo Cells At Low Dose. *Radiat. Res.* **284**, 70-77, 1995.

Miller, A.C., Ainsworth, E.J., Lui, L., Wang, T.J., and Seed, T.M., Development of Chemopreventive Strategies for Radiation-Induced Cancer: Targeting Radiation-Induced Genetic Alterations. International Conference on Low-Level Radiation Injury and Medical Countermeasures, AFRRI, 1999.

Morgan, W.F., Day, J.P., Kaplan, M.I., McGhee, E.M., and Limoli, C.L., Genomic Instability Induced by Ionizing Radiation. *Radiat. Res.* **146**, 247-258, 1996.

NASA Special Publication, Human Exploration of Mars: The Reference Mission of the NASA Mars Exploration Study Team, NASA-SP 6107, 1997

National Academy of Sciences National Research Council, Radiobiological Factors in Manned Space Flight, Washington D.C., Publications 1487, 1967.

National Academy of Sciences National Research Council, Radiation Protection Guides and Constraints for Space-Mission and Vehicle-Design Studies Involving Nuclear System, Washington D.C., 1970.

National Academy of Sciences Space Science Board, HZE Particle Effects in Manned Space Flight, National Academy of Sciences U.S.A. Washington D.C., 1973.

National Academy of Sciences, NAS. National Academy of Sciences Space Science Board, Report of the Task Group on the Biological Effects of Space Radiation. Radiation Hazards to Crews on Interplanetary Mission National Academy of Sciences, Washington, D.C., 1997.

National Council on Radiation Protection and Measurements, NCRP. Guidance on Radiation Received in Space Activities, NCRP Report **98**, NCRP, Bethesda, M.D., 1989.

National Council on Radiation Protection and Measurements, NCRP, A Guide for Uncertainty Analysis in Dose and Risk Assessments Related to Environmental Contamination. NCRP Commentary No. **14**, Bethesda, M.D., 1996.

National Council on Radiation Protection and Measurements, NCRP. Uncertainties in Fatal Cancer Risk Estimates Used in Radiation Protection, NCRP Report **126**, NCRP, Bethesda, M.D., 1997.

National Council of Radiation Protection and Measurements, NCRP. Relative Biological Effectiveness of Radiations of Different Quality, NCRP Report **104**, NCRP, Bethesda, M.D., 1990.

National Council on Radiation Protection and Measurements, Recommendations of Dose Limits for Low Earth Orbit. NCRP Report **132**, Bethesda MD, 2000.

Nelson, G., Schubert, W.W., Marshall, T.M., Benton, E.R., and Benton, E.G., Radiation Effects in Caenorhaditis Elegans: Mutagenesis by High and Low-LET Ionizing Radiation. *Mut. Res.* **212**, 181-192, 1989.

Nikjoo, H., O'Neill, P., Goodhead, D.T., and Terissol M., Computational Modeling of Low Energy Electron Induced DNA Damage by Early Physical and Chemical Events, *Int. J. Radiat. Biol*. **71**, 467-483, 1997.

Nikjoo, H., Khvostunov I.K., and Cucinotta, F.A., The Response of (TEPC) Proportional Counters to Heavy Ions, *Radiat. Res*. (submitted), 2001.

Pence, B.C., and Yang, T.C., Antioxidants: Radiation and Stress, In Nutrition in Space-flight and Weightlessness Models, Edited by H.W. Lane and D. A. Schoeller, CRC Press, 1999.

Peterson, L.E. and Cucinotta, F.A.: Monte-Carlo Mixture Model of Lifetime Cancer Incidence Risks for Radiation on Shuttle and International Space Station, *Mut. Res* **430**, 327-335, 1999.

Pierce, D.A., Shimizu, Y., Preston, D.L., Vaeth, M., and Mabuchi, K., Studies of the Mortality of the Atomic Bomb Survivors, Report 12, Part I. Cancer: 1950-1990. *Radiat. Res.* **146**, 1-27, 1996.

Polyak, K., Xia, Y., Zweiger, J.L., Kinzler, K.W., Vogelstein, B., A Model for p53-Induced Apoptosis. *Nature* **389**, 300-305, 1997.

Preston, D.L., Kusumi, S., Tomonaga, M., Izumi, S., Ron, E., Kuramoto, A., Kamada, N., Dohy, H., Matsui, T., Nonaka, H., Thompson, D.E., Soda, M., and Mabuchi, K., Cancer Incidence Studies in Atomic Bomb Survivors. Part III: Leukemia, Lymphoma and Multiple Myeloma, 1950-1987. *Radiat. Res.* **137**, S68-S97; 1994.

Rabin, B.M., Joseph, J.A., Shukitt-Hale, B., and McEwen, J., Effects of Exposure to Heavy Particles on a Behavior Medicated by the Dopaminergic System. *Adv. Space Res.* **25**, (10) 2065-(10) 2074, 2000.

Sasaki, M.S., Takatsuji, T., Ejima, Y., The F Value Cannot be Ruled out as a Chromsal Figureprint of Radiation Quality. *Radiat. Res.* **150**, 253-258, 1998.

SEER Stat Version 2.0, Cancer Statistics Branch, National Cancer Institute, Bethesda, M.D., 1999

Simonsen, L.C., Wilson, J.W.,Kim, M.H., and Cucinotta, F.A., Radiation Exposure for Human Mars Exploration, *Health Phy.,* **79** (5), 515-525, 2000.

Sinden, R., Pearson, C.E., Potaman, V.N., and Ussery, D.W., DNA: Structure and Function. In Advances in Genome Biology Volume 5A (editor R.S. Verma) JAI Press, 1998.

Smart, D.F. and Shea, M.A., Modeling the Time Intensity Profiles of Solar Flare Generated Particle Fluxes in the Inner Heliosphere. *Adv. Space. Res.* **12**, 303-313, 1992.

Smith, D.E., Zuber, M.T., Solomon, S.C., Philips, R.J., Head, J.W., Garvin, J.B., *et al.,* The Global Topography of Mars and Implications for Surface Evolution, *Science* **284**, 1495-1503, 1999.

Storer, J.B., and Mitchell, T.J., Limiting Values for the RBE of Fission Neutrons at Low Doses for Life Shortening in Mice. *Radiat. Res.* **97**, 396-406, 1984.

Storer, J.B., and Fry, R.J.M., On the Shape of the Neutron Dose-Effect Curves for Radiogenic Cancers and Life Shortening in Mice, *Radiat. Env. Biophys.* **34**, 21-27, 1995.

Strauss, M., Lukas, J., and Bartek, J., Unrestricted Cell Cycling and Cancer, *Nature Med.,* **1**, 1245–1256, 1995.

Taccioli, G.E., Rathbun, G., Oltz, E., Stamato, T., Jeggo, P.A., and Alt., F.W., Impairment of V(D)J Recombination in Double-Strand Break Repair Mutants. *Science*, **260**, 207-210, 1994.

Thompson, D.E., Mabuchi, K., Ron, E. Soda, M., Tokunaga, M., Ochikubo, S., Sugimoto, S., Ikeda, T., Terasaki, M., Izumi, S., Preston, D.L.. Cancer Incidence Studies in Atomic Bomb Survivors, Part II: Solid Tumors, 1958-1987. *Radiat. Res.,* **137**, S17-S67, 1994.

Todd, P., Stochastics of HZE-Induced Microlesions. *Adv. Space Res.*, **9**, (10) 31-(10) 34, 1981.

Todd, P., Percent, M.J., Fleshner, M., Combined Effects of Space Flight Factors and Radiation on Humans, *Mutation Res.*, 211-219, 1999.

Tolifon, P.J., and Fike, J.R., Review: The Radioresponse of the Central Nervous System: A Dynamic Process. *Radiat. Res.* **153**, 357-370, 2000.

Ullrich, R.L., Tumor Induction in BAL/c Mice After Fractionated Neutron or Gamma Irradiation. *Radiat. Res*. **93**, 506-512, 1984.

Ullrich, R.L., and Ponnaiya B., Radiation-Induced Instability and its Relation to Radiation Carcinogenesis, *Inter. J. Radiat. Biol.* **74**, 747-754,1998.

Vogelstein, B., and Kinzler, K.M., The Genetic Basis of Human Cancer, McGraw-Hill, New York, 1997.

Williams, J.R., Zhang, Y., Zhou, H., Osmana, M., Cha, D, Kavet A., Cucinotta, F.A., Dicello, J.F., and Dillehay, L.E., Predicting Cancer Rates in Astronauts From Animal Carcinogenesis Studies and Cellular Markers, *Mut. Res.* **430**, 255-269, 1999.

Wilson, J.W., L.W. Townsend, W. Schimmerling, G.S. Khandelwal, F. Khan, J.E. Nealy, F.A. Cucinotta, L.C. Simonsen, and J.W. Norbury, Transport Methods and Interactions for Space Radiations, RP1257, NASA, Washington D.C., 1991.

Wilson, J. W., Kim, M., Schimmerling, W., Badavi, F. F., Thibeault, S. A., Cucinotta, F. A., Shinn, J. L., and Kiefer, R., Issues in Space Radiation Protection, *Health Phys*. **68**, 50-58, 1995.

Wilson, J.W., Cucinotta F.A., Shinn J.L., Simonsen L.C., Dubey R.D., Jordon W.R., Jones J.D., Chang C.K., and Kim M.Y., Shielding from Solar Particle Event Exposures in Deep Space. *Radiat. Meas.* **30**, 361-382, 1999a.

Wilson, J.W., Kim M.Y., Shinn J., Tai H., Cucinotta F.A., Badhwar G.D., Badavi F.F., Atwell W.: Solar Cycle Variation and Application to the Space Radiation Environment. NASA TP 209369, 1999b.

Wolfe, C., Lafuma J., Masse, R., Morin M., and Kellerer, A.M., Neutron RBE for Induction of Tumors With High Lethality in Sprague-Dawley Rats. *Radiat. Res.* **154**, 412-420, 2000.

Yucker, W.R., Huston, S.L., Reck, R.J., Computerized Anatomical Female, McDonnell Douglas Space System Company, MDC-H-6170, 1990.

APPENDIX-A

MECHANISMS AND BIOLOGICAL EFFECTS OF HEAVY IONS AND ALTERNATIVE RISK SYSTEMS

As a particle passes through tissues, cells, or DNA, ionization events on biomolecules occur leading to the production of secondary electrons. Close to an ion track, particles directly excite biomolecules. Lower energy electrons produced in these events deposit a large amount of energy, however are confined to a small radial region about the ion track in the so called track core. Higher-energy electrons ejected by the ion are termed ŭ-rays and impart energy in other areas of the cell or even in adjacent cells (**Figure- 2a**). The term track structure refers to the description of the spatial distribution of energy deposition events at the biomolecular level. The variations in radial dose across the cell are large and are an illustration of heterogeneity in energy deposition within a cell for ions, which contrasts strongly with photon irradiation. **Figure-22** illustrates this heterogeneity for a plane of cells bombarded with 20 MeV/u iron ions. In analogy to the macroscopic dose, the mean specific energy is defined as the average energy deposited in a microscopic volume divided by the mass of the molecular volume being considered. Table 2 shows evaluations of the mean specific energy by photons, protons and heavy ions in a small segment of DNA, a DNA nucleosome (160 base-pairs (bp)), a segment of the DNA fibre (1000 bp), and the cell nucleus. Extremely large values occur due to the small volumes being considered. The energy deposition in biomolecules is a stochastic quantity and average values provide only limited information, the spectrum of energy deposition events provides a more useful analysis tool. Examples of such spectrum for a DNA nucleosome are shown in Figure 2b for several radiation types (Cucinotta *et al*., 2000b). The left hand side shows the absolute probability of depositing energy in the nucleosome and the right hand side scales by the number of nucleosomes per mammalian cell (2.9×10^7) to show the frequency at which events occur.

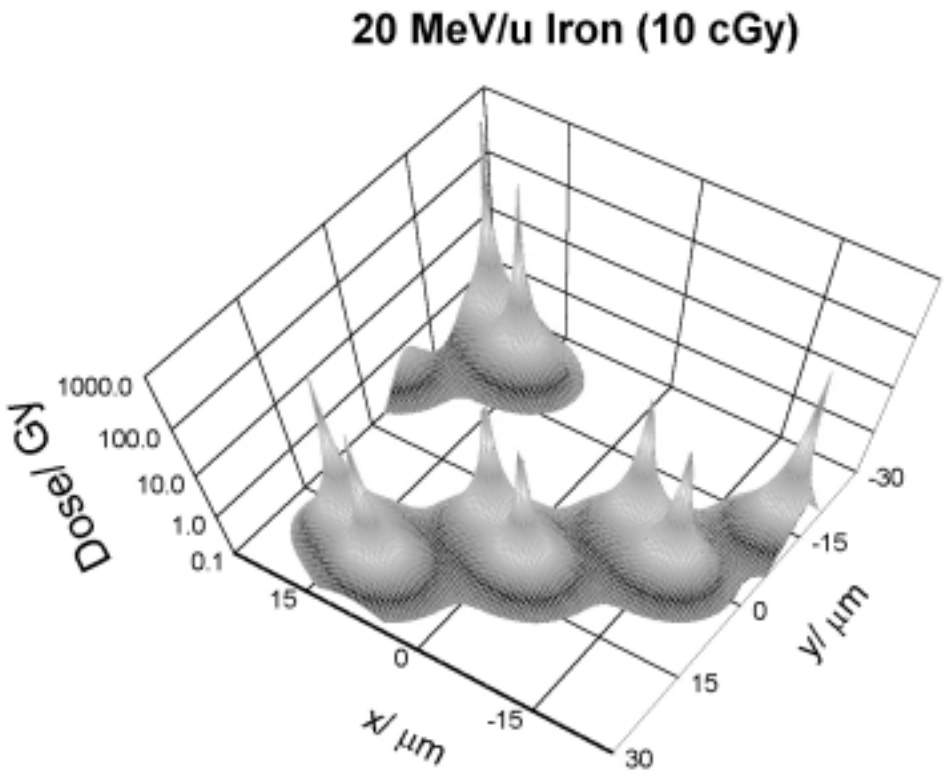

Figure 22: Calculations of random tracks of 20 MeV/u ^{56}Fe passing through a plane of cells of 15 µm diameter. The combined radial dose contributions from several tracks are plotted to illustrate the spatial distribution. [data from Cucinotta *et al.,* 1999a]

Radiation produces DNA damage leading to cellular effects through both direct ionization of molecules or through the diffusive action of radicals. Radical production occurs predominantly on water molecules because of their abundance in cells. For understanding DNA damage, the structure of the hydration shell that surrounds and interacts with DNA and histone proteins is important (Nikjoo *et al*., 1997). In vivo, radical diffusion lengths are small which has led to the understanding that radicals makeup only a minor contribution in DNA damage, especially for high-LET radiation. Direct interaction with DNA or hybrid damage involving both radical and direct DNA damage are the predominate modes of DNA damage *in vivo* (Nikjoo *et al.,* 1997). Damage to DNA consists of ruptures in the sugar-phosphate backbone of DNA denoted as single-strand breaks (SSB) or if on both DNA strands they are

denoted as double-strand breaks (DSB). Other types of DNA damage include base-damage (BD) and DNA-protein cross-links involving predominantly DNA and histone proteins. The number of SSB or DSB breaks produced by radiation varies little with radiation type and about 2000 SSB and 30 DSB, respectively are produced for each Gy of radiation in mammalian cells. The most important type of damage to DNA at low dose-rates may be complex or clustered DNA damage which consists of mixtures of two or more of the various types of damages (SSB, DSB, etc.) within a localized region of DNA. The frequency and severity of clustered damage increases with LET and it is expected that very little repair of clustered damage occurs and rather un-repairable damage is produced leading to small interstitial deletions or chromosome aberrations that contribute to gene mutations or cell death. Table-16 shows results of Monte-Carlo simulations for the fractional contribution of several classes of DNA break for different types of radiation (Nikjoo *et al.,* 1997). The simulations include molecular descriptions of DNA and its hydration shell and radical diffusion processes. Breaks with one or more associated breaks nearby are described with a '+' and '++' superscript for one or two associated damages, respectively. A 10-100-fold higher probability per unit dose of complex breaks for high-LET radiation compared to low-LET radiation occurs. The energy imparted to the nucleosome for these complex break types is above 100 eV and from Figure 2b we observe the much higher occurrence of these events for high-LET radiation. New experimental techniques are being developed to measure complex DNA damages and their repair (Lobrich, *et al.,* 1995) and are providing validation of the theoretical prediction that complex DNA damage is the chief mechanism for the large biological effectiveness of high-LET radiation compared to photons. An unexplored area are possible differences in initial biochemical species produced in the cytoplasm and nuclear matrix for high and low-LET radiation and their potential role in deleterious health effects.

Radiation	SSB	SSB+	2SSB	DSB	DSB+	DSB++	No-break
Electron (5 keV)	23%	1.9	0.3	1.2	0.3	0.005	73.3
Proton (1 MeV)	25	2.6	0.9	2.7	1.2	0.22	66.4
Alpha (2 MeV)	26.4	7.2	1.5	4.8	3.6	1.3	55.2

Table 16: Percent contributions for distinct DNA break types for various radiations interacting with a DNA nucleosome [Nikjoo and Goodhead, 1998].

Several DNA damage processing or repair processes exist in cells to respond to damage from radiation. In general DNA repair involves the three steps of damage recognition, removal of damaged molecules, and synthesis and rejoining. Base damage is repaired by excision repair pathway where damaged or inappropriate bases are excised and replaced by the correct nucleotide sequence. In mammalian cells, the nucleotide excision repair pathway has been well studied with many of the gene products involved in the kinetic steps of DNA incision, removal of bases, and synthesis now well characterized (Friedberg *et al.,* 1995). The mismatch base repair pathway functions to correct errors in opposite base pairs. Such errors occur with a small probability during DNA replication and has been shown to be especially important in the long tandem DNA repeats that occur in satellite DNA (Sinden, *et al.,* 1998). Mutations or deletions of genes that function in mismatch base repair have been found to be important in some forms of hereditary cancers including colorectal cancer. The repair of single strand breaks can be made directly through ligation of the ends if there is no associated base damage and thus avoids the need for the DNA synthesis step.

The repair of DSB's is known to occur through direct end-joining and homologous recombination processes. Recent studies have indicated that these pathways are conserved from yeast to mammalian cells (Kanaar and Hoeijmakers, 1997). The availability of individual processing pathways may be dependent on cell-cycle phase and tissue type (Kanaar and Hoeijmakers, 1997). Homologous recombination involves processing of damaged DNA ends, branch migration, formation of Holiday junctions, DNA synthesis, and restitution. Many of the gene products that participate in homologous and non-homologous recombination have now been identified (Kannar and Hoeijmakers, 1997). Homologous recombination with undamaged DNA on a sister chromatid or other chromosomes with limited homology may be less error-prone than NHEJ, however the repair efficiency of these processes has not been well established. For high-LET radiation where complex DSBs occur with large frequency, little repair occurs possibly leading to cell death or that unrepairable ends are rejoined with other radiation induced DSBs leading to large DNA deletions and chromosome aberrations.

Mutation types produced by radiation include point mutations where base changes leading to alterations in gene function occur, insertions where aberrant DNA is inserted within a gene, deletions where genes lose function or are totally lost, and chromosome aberrations involving mis-joining or deletion of large segments of chromosomes. Radiation is extremely effective at producing large-scale deletions and chromosomal aberrations. An important role is expected for mutations to non-essential DNA. Such mutations do not directly effect gene function, however are believed to lead to replication errors. The mutation spectrum produced by heavy ions have been shown to be effected by cell type, DNA repair and signaling genes (Taccioli *et al.,* 1993; Chernbonnel-Lasserre, *et al.,* 1996), and particle fluence. An important consideration of heavy ions is the role of cell death since only surviving cells can express a mutant phenotype. Since low doses of heavy ions can lead to cell death, the expression of mutations is reduced for heavy ions with large charge numbers (Cucinotta *et al.,* 1996). Only a few gene loci have been studied with HZE particles for mutation rates these include the heterozygous HPRT locus (Kiefer, *et al.,* 1994) and the autosomal TK locus (Kronenberg and Little, 1989). Nelson *et al.,* (1989) studied mutation induction at several loci with heavy ion beams in *C. elegans*.

Genomic Instability and Cancer

The latency period for carcinogenesis varies from several years to more than 30 years after exposure to radiation. Because of this long latency and the observed increase with age for the appearance of cancers in the general population, it had been long suspected that cancer involves the accumulation of many genetic changes. The development of new molecular techniques in the 1980s confirmed this view and it is found that from at least 4 to more than 10 genetic alterations are involved in the development of most non-hereditary cancers. Based on known mutation rates for various carcinogens, there is an extremely small probability that such a large number of genetic alterations could be formed independently. Instead, it is now believed that a kind of instability is induced by carcinogens through either genetic or epigenetic mechanisms (Morgan *et al.*, 1996). This area of research has been denoted as genomic instability and in the field of radiobiology involves the study of delayed effects in the progeny of irradiated cells including chromosome aberrations, mutations, cell death, and persistent reactive oxidative damage (ROS).

Cytogenetic approaches have been used extensively for understanding genomic instability and have begun to define relationships to carcinogenesis. Khadim *et al.* (1992) observed instability in the form of delayed chromatid aberrations in primary bone marrow stem cells using high-LET alpha particle irradiation. An increase in the number of aberrations for more than 30 cell divisions from radiation exposure was found with alpha particles, however instability was not found following x-ray exposures. Another study by Ullrich and Ponnaiya (1998) has used mouse mammary stem cells irradiated *in vivo* and observed chromatid type aberrations for up to 40 cells division after neutron irradiation. These studies also considered mutations in the p53 and pRB genes. These genes are mutated or functional inactivated in more than 50% of human cancers (Strauus, *et al.*, 1995). The studies of Ullrich and Ponnaiya (1998) have shown that although p53 was inactivated in many clones, it was a primary event in only a small number of cases and rather was induced as subsequent event by some other factor caused by radiation. Gene mutation rates have a probability of about 10^{-5} to 10^{-4} per cell per Gy, which suggests that mutations are not the primary event for instability in most cases. This is supported by the studies of Khadim *et al.* (1992), which showed that instability was induced in about 3 of 10 surviving cells following high-LET alpha particle irradiation of primary bone marrow stem cells. Such research is showing important similarities for the dose-response from cytogenetic observations associated with instability and previous studies of cancer induction in animals including a strong correlation between radiation sensitivity, cancer induction and chromosomal instability in the mouse (Ullrich and Ponnaiya, 1998). The bending of the response for tumor induction or chromosomal instability as the dose or fluence is increased has been attributed to the role of cell killing, the inherent susceptibility of a population, and more recently, genomic instability leading to a higher fraction of lethal aberrations at higher doses. An understanding of such mechanisms is important.

A precise causal mechanism for genomic instability has not been established (Morgan, *et al.*, 1996). Areas of focus include persistent reactive oxidative damage (ROS), and the role of errors in DNA synthesis due to radiation induced small interstitial deletions in non-essential DNA. It is also postulated that damage to extra-cellular matrix by high-LET radiation (Barcellos-Hoff, *et al*., 1998) may lead to instability in progeny cells. Another mechanism currently being explored in mutation and instability studies is the role of bystander effects

where extra-cellular factors or aberrant cell signaling effects in "hit" cells produce these outcomes in neighboring "un-hit" cells (Desphande, *et al.,* 1996). Finally, the possibility of mutations in one or more of the many genes involved in DNA repair and cell cycle regulation cannot be excluded. A challenge for the future will be the development of biologically based risk assessment models that includes mechanisms of radiation action that have been described experimentally.

Because of the revolution in molecular biology over the last 15 years, it is expected that new approaches to estimate risk will be forthcoming (LBNL, 1997). These include the use of transgenic or knockout mice, and new cellular assays including *in-vivo/in-vitro* models. One approach described above is the study of genomic instability using cytogenetic techniques. Other possibilities could include studies of gene amplification, loss of apoptosis, loss of cell controls as observed in the progenies of irradiated cells (or other delayed events known to occur in the carcinogenesis process). Large-scale cDNA arrays are now capable of correlating the responses of over 20,000 genes as a function of exposure type. Such technology is expected to lead breakthroughs in the future (DeRisi *et al.,* 1997; Fornace *et al.,* 1999). Although some work in these areas have been reported in the scientific literature, the quantitative estimate of risk using such approaches have not been realized at this time.

The development of theoretical models of risk should be one goal of future research aimed at risk estimation. The value of such models would be in providing quantitative descriptions where the weight of experimental knowledge and epidemiological data were being put forth in the risk projection while providing tools for both extrapolation and predictive assessments. Frequently used epidemiological models of cancer risks such as the relative risk model for solid tumors or the additive risk model for leukemia already contain some assumptions of the underlying processes and have advantage of inclusion of background incidence rates as a function of age and sex. Future risk assessment approaches could improve on these models by avoiding the use of dose and RBEs in describing radiation effects and instead incorporate knowledge of particle tracks (Nikjoo *et al.,* 1997), the kinetics of DNA recombination (Cucinotta *et al*., 2000c), cell cycle regulation (Cucinotta and Dicello, 2000d) and mechanisms of the initiation and promotion that contribute to cancer progression.

APPENDIX-B

CRITICAL QUESTIONS FOR RADIOBIOLOGY RESEARCH

This appendix lists critical questions in radiobiology research gathered from previous NASA Radiation Health Program's Annual Investigator Meetings and Workshops.

Space Radiation Environment

- For a given mission, what are the fluxes of GCR in interplanetary space as a function of particle energy, LET, and solar cycle?
- What is the solar cycle dependence of space radiation?
- What is the trapped radiation flux as a function of time, magnetic field coordinates and geographical coordinates?
- What are the maximum flux, the integrated fluence, and the probability of large Solar Particle Events (SPE) during any mission?
- What are the doses related to heavy ions in deep space?
- What are the factors that determine radiation flux of SPE?

Nuclear Interactions

- What are the cross sections and yields for nuclear interactions of HZE particles in tissue and shielding materials?
- What are the angular distributions of nuclear interaction products?
- What are the particle multiplicities of nuclear interaction products?
- How is a radiation field transformed as a function of depth in different materials?
- What are the optimal ways of calculating the transport of radiation through materials?

Atomic Interactions

- What is the precise energy deposition of heavy ions?
- What are the yields and energy spectra of electrons?
- How can the wealth of knowledge existing for energy deposition in gaseous media be extended to the liquid phase applicable to most living cells?
- How do diffusion, recombination and other interactions of chemical intermediaries alter the chemical events at the DNA level?
- How is physical energy deposition related to biological effect?

Molecular Biology

- What are the probabilities of GCR to produce radiation damage at specific sites and of specific types on DNA?
- How are processes like oncogene activation and oncogene suppressor inactivation involved in the carcinogenic effects of GCR radiation?
- What mechanisms are involved in modulating radiation damage at the molecular level (DNA recombination or repair, errors in repair, gene amplification, etc.)?
- How can molecular mechanisms of radiation damage be used to understand effects in whole cells?
- What role does oxidative or other damage to non-DNA targets play in carcinogenesis or other late effects?
- Are DNA recombination processes observed at high dose-rates the same at low dose-rates?

Cellular Biology

- What is the probability of initiating neoplastic cell transformation or other steps leading to a cancerous cell?

- How do cellular repair mechanisms modulate damage produced by energetic charged particles? How can the radiation effects on cells in culture be related to radiation effects in "normal" cells and tissues?
- How can cellular mechanisms of radiation damage be used to understand effects in whole organisms?

Damage to the Central Nervous System

- Are there significant behavioral consequences of radiation exposure from protons? Heavy ions?
- Is there significant loss in the CNS from passage of protons and heavy ion tracks on long deep space missions?
- What is the role of the vasculature in CNS injury?
- What is the functional significance of simultaneous stimulation, damage, or inactivation of sets of cells along a particle track?
- What is known about hereditary predisposition to radiation or oxidative stress injury?
- What are the most important types of cells in radiation damage? Neurons? Axons?
- What is the latency of CNS injury?
- Is damage to the CNS reversible?

Animal Models

- How can animal models be used to extrapolate probabilities of radiation risk to humans in space?
- What is the relative biological effectiveness of different types of radiation for the relevant endpoints such as cancer; cataracts?
- How can protection against the effects of galactic cosmic rays and the proton radiation of solar events be improved?

- What is the age dependence of relevant radiation effects in animals (cancer, cataractogenesis, life shortening, etc.)?

Extrapolation to Humans

- What should be the radiation "dose limits" for manned deep space missions?
- What is the probability of cancer as a function of dose, dose rate, radiation quality, gender, age at exposure, and time after exposure?
- What is the effect of GCR at different stages of the carcinogenesis process?
- What is the probability of cataract formation as a function of the same quantities?
- What is the probability for genetic and developmental detriment incurred as a consequence of radiation exposure in space?
- Are lifetime cancer risks be used for high-LET radiation or should age-specific risks be used because of the shorter latency time observed in animal models?
- How are risks associated with acute exposure to space radiation to be managed medically?
- How a probabilistic model of CNS injury can be developed?
- What pharmacological agents should be developed and tested as prophylactic agents for low-LET?
- What will the radiation environment be within the space vehicle and what factors influence the flux, energy, and linear energy transfer spectra of the radiation?